

MicroRNA profiles associated with bone healing of the extraction socket in
bisphosphonate related osteonecrosis of the jaw in rat model



A Thesis Submitted in Partial Fulfillment of the Requirements
for the Degree of Master of Science in Geriatric Dentistry and Special Patients Care

Common Course

FACULTY OF DENTISTRY

Chulalongkorn University

Academic Year 2020

Copyright of Chulalongkorn University

รูปแบบไมโครอาร์เอ็นเอที่เกี่ยวข้องกับการหายของแผลถอนฟันในหนูที่มีภาวะกระดูกตายที่สัมพันธ์
กับการใช้ยาบิสฟอสโฟเนต



วิทยานิพนธ์นี้เป็นส่วนหนึ่งของการศึกษาตามหลักสูตรปริญญาวิทยาศาสตรมหาบัณฑิต
สาขาวิชาทันตกรรมผู้สูงอายุและการดูแลผู้ป่วยพิเศษ ไม่สังกัดภาควิชา/เทียบเท่า
คณะทันตแพทยศาสตร์ จุฬาลงกรณ์มหาวิทยาลัย
ปีการศึกษา 2563
ลิขสิทธิ์ของจุฬาลงกรณ์มหาวิทยาลัย

ฐาปกรณ์ สุรจกุลวัฒนา : รูปแบบไมโครอาร์เอ็นเอที่เกี่ยวข้องกับการหายของแผลถอนฟันในหนูที่มีภาวะกระดูกตายที่สัมพันธ์กับการใช้ยาบิสฟอสโฟเนต. (MicroRNA profiles associated with bone healing of the extraction socket in bisphosphonate related osteonecrosis of the jaw in rat model) อ.ที่ปรึกษาหลัก : ผศ. ทญ. ดร.สุปรีดา ศรีธัญรัตน์, อ.ที่ปรึกษาร่วม : ผศ. ทญ. ดร.อัญชลี วัชรรักษะ

บิสฟอสโฟเนตถูกใช้ยาเพื่อรักษาโรคกระดูกพรุน มะเร็งเม็ดเลือด มะเร็งเต้านม และมะเร็งกระดูกที่ลุกลามอย่างแพร่หลาย หากผู้ป่วยที่ได้รับยาดังกล่าวมีอันตรายต่อการขากรรไกร หรือการถอนฟันจะเหนียวนำไปให้เกิดภาวะกระดูกขากรรไกรตายที่สัมพันธ์กับการใช้ยา เนื่องจากกลไกของยาจะไปขัดขวางกระบวนการหายของกระดูกและการสร้างหลอดเลือดใหม่ เมื่อกระดูกขากรรไกรตายเกิดขึ้น การดูแลรักษาให้หายขาดเป็นไปได้ยากและส่งผลกระทบต่อคุณภาพชีวิตที่แย่งลงของผู้ป่วย การนำไมโครอาร์เอ็นเอมาใช้ในการรักษาโรคต่างๆเป็นสิ่งที่น่าสนใจในทางการแพทย์ โดยมีจุดประสงค์เพื่อหาบทบาทที่สำคัญของไมโครอาร์เอ็นเอต่อการก่อโรคภาวะกระดูกตายที่สัมพันธ์กับการใช้ยา

วิธีการ หนู 17 ตัวแบ่งเป็น 2 กลุ่ม กลุ่มที่1 ฉีดยาโซลิโดรเนตร่วมกับเดกซาเมทาโซนเป็นกลุ่มทดลอง กลุ่มที่2 ฉีดน้ำเกลือเป็นตัวแปลควบคุม ภายหลังจากฉีดยา 2 สัปดาห์ ถอนฟันกรามบนซี่ที่1 ทั้ง 2 ข้าง สังเกตภาวะกระดูกขากรรไกรตายที่สัมพันธ์กับการใช้ยาหลังจากถอนฟันหนูโดยประเมินจาก ลักษณะทางคลินิก ภาพถ่ายรังสีเครื่องเอกซเรย์คอมพิวเตอร์ระดับไมโครเมตร และการวิเคราะห์ทางมิถุนวิทยา หลังจากถอนฟันหนู 28 วัน เก็บชิ้นเนื้อกระดูกในแผลถอนฟันตัวอย่างเพื่อวิเคราะห์ทางไมโครอาร์เอ็นเอ

ผลการศึกษา ในการทดลองนี้สามารถทำให้เกิดภาวะกระดูกขากรรไกรตายที่สัมพันธ์กับการใช้ยาในกลุ่มทดลองได้สำเร็จ พบไมโครอาร์เอ็นเอที่มีผลต่อการเกิดภาวะกระดูกขากรรไกรตายที่สัมพันธ์กับการใช้ยา ไมโครอาร์เอ็นเอที่มีผลขัดขวางการสร้างกระดูกคือ ไมโครอาร์เอ็นเอ-23a-3p, ไมโครอาร์เอ็นเอ-23b-3p, ไมโครอาร์เอ็นเอ-27a-3p และไมโครอาร์เอ็นเอ-24-3p ไมโครอาร์เอ็นเอที่มีผลส่งเสริมการสร้างหลอดเลือดคือ ไมโครอาร์เอ็นเอ-663a และไมโครอาร์เอ็นเอ-720 ไมโครอาร์เอ็นเอที่เกี่ยวข้องทั้งการสร้างกระดูกและการสร้างหลอดเลือดคือ ไมโครอาร์เอ็นเอ-34a

สรุปผลการศึกษา การศึกษานี้แสดงบทบาทของไมโครอาร์เอ็นเอที่ควบคุมเซลล์ที่เกี่ยวข้องกับกลไกการสร้างกระดูกและหลอดเลือดที่ส่งผลให้เกิดภาวะกระดูกขากรรไกรตายที่สัมพันธ์กับการใช้ยา

สาขาวิชา	ทันตกรรมผู้สูงอายุและการดูแลผู้ป่วยพิเศษ	ลายมือชื่อนิสิต
ปีการศึกษา	2563	ลายมือชื่อ อ.ที่ปรึกษาหลัก
		ลายมือชื่อ อ.ที่ปรึกษาร่วม

ACKNOWLEDGEMENTS

The authors thank the Immunology Laboratory, Department of Periodontology and the Department of Microbiology, Faculty of Dentistry, Chulalongkorn University for providing laboratory facilities and technical support. We are also thankful to the Chulalongkorn University Laboratory Animal Center (CULAC) for experiment facility and veterinary supports. This study was funded by Chulalongkorn University; Grant Number CU_GR_62_78_32-02.

Thapakorn Surajkulwatana



TABLE OF CONTENTS

	Page
ABSTRACT (THAI).....	iii
ABSTRACT (ENGLISH).....	iv
ACKNOWLEDGEMENTS	v
TABLE OF CONTENTS	vi
LIST OF TABLES.....	ix
LIST OF FIGURES	x
Chapter 1.....	12
Introduction	12
Background and rationale	12
Research objective.....	13
Hypothesis.....	14
Field of research	14
Limitation of research.....	14
Application and expectation of research.....	14
Key words	14
Conceptual Framework	15
Chapter II.....	16
Literature review.....	16
1. MRONJ definition.....	16
2. Burden of disease	16
3. Incidence of MRONJ	16

4. Risk factor of MRONJ	17
5. Bisphosphonates (BPs).....	17
5.1 The benefits of bisphosphonates.....	17
5.2 Drug administration.....	18
6. Treatment of MRONJ.....	20
7. microRNAs	21
7.1 Role of miRNAs in the pathogenesis of MRONJ.....	21
7.1.1 Angiogenesis-regulatory miRNAs.....	21
7.1.2 Bone remodeling-regulatory miRNAs.....	29
Repress expansion and lineage direction and limit bone mass	34
Chapter III	36
Research and methodology	36
The animal experiment	36
Body weight evaluation.....	37
Gross and radiographic evaluation	37
Micro-CT analysis.....	38
Histological analysis.....	39
miRNA analysis.....	39
Statistical analysis	40
Chapter IV.....	43
Results.....	43
Animal model.....	43
Changes in body weight	43
Gross and radiographic evaluation	44

Micro-CT analysis.....	46
Histological analysis.....	47
miRNA analysis.....	49
Chapter V.....	51
Discussion.....	51
Chapter VI.....	55
Conclusion.....	55
Appendix.....	56
Information of animal model.....	56
Body weight (g) : lot 2 only.....	56
Protocol Drug injection.....	57
General anesthesia before operation.....	58
Protocol for blood withdrawal.....	59
Cardiac puncture.....	59
Gross, micro-CT and histological data.....	61
Results in PCRArray.....	65
miRNA concentration from Nanodrop (Bone).....	66
Result micro – CT (bone volume).....	70
Statistics.....	71
REFERENCES.....	72
VITA.....	84

LIST OF TABLES

	Page
Table 1. Angiogenesis-regulatory miRNAs and their targets (Wu et al., 2009).	22
Table 2. miRNAs and their targets involved in the pathogenesis of MRONJ in review literature.....	32
Table 3. List of candidate miRNAs in MRONJ rat model.....	41
Table 4. Designed primer of candidate miRNAs.....	42



LIST OF FIGURES

	Page
Figure 1 Biogenesis of angiogenesis-related miRNAs (Wu et al., 2009).....	22
Figure 2 miR-720 pathway that promote endothelial cell activity (Wang et al., 2014).	24
Figure 3 Target protein of miRNA in non-endothelial cell. (Wang and Olson, 2009). ..	25
Figure 4 Target protein of miRNAs in endothelial cell (Wang and Olson, 2009).....	27
Figure 5 <i>RBP2/NOTCH1/CYCLIN D1</i> collaboration in osteogenic acitivity (Fan et al., 2016).....	29
Figure 6 Experimental diagram and timeline.....	37
Figure 7 Setting of the region of interest (ROI) and volume of interest (VOI) in an extraction socket	38
Figure 8 Setting of the region of interest (ROI) for histological analysis in extraction socket.....	39
Figure 9 Change in mean body weight at baseline, Day (-7), 0, 7, 14, and 28 of tooth extraction; normal saline administration (NSS), zoledronate and dexamethasone administration (Zol), and total (n=10).....	44
Figure 10 Gross evaluation: 14 and 28 days after extraction, (A) normal saline (NSS) group at day 14, (B) NSS group at day 28, (C) zoledronate and dexamethasone administration (Zol) group at day 14, and (D) Zol group at day 28.....	45
Figure 11 Micro-CT views: 14 and 28 days after extraction, (A) normal bone healing in NSS group at day 14, (B) normal bone healing in NSS group at day 28, (C) showed delayed bone healing in the extraction sockets of Zol group at day 14, (D) showed delayed bone healing in the extraction sockets of Zol group at day 14.	45
Figure 12 % Bone exposure occurrence (N= 14) : 14 and 28 days after extraction.....	45

Figure 13 μ CT imaging demonstrated three-dimensional (3D) of volume of interest (VOI) size $0.5 \times 0.5 \times 0.5 \text{mm}^3$. (A) normal saline administration (NSS-28), (B) zoledronate plus dexamethasone administration (Zol-28).....	46
Figure 14 New bone formation (mm^3) at Day 28 after extraction analyzed by μ CT in each group (data calculated per socket; n=12).	47
Figure 15 Histological images demonstrated complete epithelial lining and bone healing was found in the control group after 28-day extraction (A). A lack of mucosal coverage in the extraction socket, abundant of infiltrated cell (arrow), and abnormal bone remodeling could be observed in Zol group after 28 days of extraction. (B); scale bar: $100 \mu\text{m}$. Enlarged images of the square areas in 10X (D-F); scale bar: 1 mm.	48
Figure 16 Percentage of bone formation cells determined at Baseline, Day 14 and Day 28 after extraction (N=17).....	48
Figure 17 Percentage of osteocyte in lacunae determined at Day 28 after extraction (N=6).....	49
Figure 18 The relative expressions of candidate miRNAs in Zol-treated group and control group (NSS-group) at Day 28 post-extraction (N=5).	50
Figure 19 The fold change miRNAs comparison between Zol-treated group and control group (NSS-group) at Day 28 post-extraction (N=5).	50

Chapter 1

Introduction

Background and rationale

Medication-related osteonecrosis of the jaw (MRONJ) occurred in patients who take antiresorptive or anti-angiogenic drugs, especially bisphosphonates (BPs), for the treatment of menopausal osteoporosis or cancer (Drake et al., 2008; McClung et al., 2013; Somerman and McCauley, 2006). Despite a minute incidence, patients who suffered from MRONJ are distressed with the symptoms such as pain, swelling, cellulites, halitosis, and trismus. Intraoral examination finds bone exposure at upper or lower jaw, pathologic fracture, oral-cutaneous fistula, or presence of infection that cause physical pain, psychological problem that effect to speech, swallowing or eating resulted in worsen quality of life (Miksdad et al., 2011; Ruggiero et al., 2014).

The use of BPs aims to abrogate metastasis of cancer via anti-angiogenesis effect and impede bone resorption activity in osteoporosis which affects through both osteoclastic and osteoblastic activity (Ruggiero et al., 2014). BPs could have anti-angiogenic activity which in turn restricted the pathway of nutrient and oxygen transportation, immune cells infiltration and also reduced serum VEGF levels (Nissen et al., 1998). BPs inhibited osteoclastic activity, which led to reducing in the activation of osteoblasts. Consequently, bone formation was arrested due to a decrease of osteoblastic activity (Ganda, 2013). These effects of BPs appeared to severely impact the wound healing of jaw bone.

Dental treatment strategy of MRONJ depends on the stage of disease. Patients who have risk of MRONJ should be monitored signs and symptoms that may occur during a treatment. The benefit of an early treatment by prescribing analgesic drugs, antibiotics, or 0.12% chlorhexidine mouthwash to the patients who have pain or

discomfort in upper or lower jaw for pain and infection control. Patients who have sequestrum and exposed bone were benefited from debridement. In some severe cases, a need to resect infected bone may offer long-term palliation with resolution of acute infection and pain. Symptomatic patients with late stage may require resection and immediate rehabilitation with a reconstruction plate or an obturator (Ruggiero et al., 2014). Although several studies have demonstrated that the surgical treatment of MRONJ was more effective than the non – surgical treatment (Graziani et al., 2012; Vescovi et al., 2011), many MRONJ patients refused to receive such invasive treatment. Therefore, the new strategies of non-invasive treatment and prevention for MRONJ are needed.

Currently, microRNAs (miRNAs) associated with many diseases are found in human genome. miRNA can regulate or fine tune the expression of DNA, resulting in protein formation or suppression of protein production (Bartel, 2004; Fish et al., 2008; Harris et al., 2008; Wu et al., 2009). The application of miRNA for curing the diseases is the forefront field in medicine presently. Accordingly, it is interesting to know whether which target miRNAs involve in the pathogenesis of MRONJ. To our knowledge, the studies related to the target miRNAs which play a role in controlling the effect of BPs to the healing of jaw bone is still lacking. This study aims to investigate the candidate miRNAs associated with MRONJ in a rat model. The future application of target miRNAs may provide a promising alternative administration for the treatment of MRONJ.

Research objective

This study aims to investigate the candidate miRNAs associated with MRONJ in a rat model. The future application of target miRNAs may provide a promising alternative administration for the treatment of MRONJ.

Hypothesis

The expression of miRNA profiles is altered during bone healing in a rat model of Medication-related osteonecrosis of the jaw compared to the normal wound healing.

Field of research

Experimental Research; In vivo study

Limitation of research

Animal experiment is essential to provide understanding of the fundamental mechanisms underlying the regulation of bone healing. One of the limiting factors in translation of knowledge from animal studies to human is the limitations of the in vivo models. Non-human animals, such as rats, are a powerful tool for providing information from a given situation in many biological pathways. However, many factors influence the process of bone healing in human, such as age, gender, genetics, soft tissue injury. Therefore, to translate this knowledge into humans required further studies.

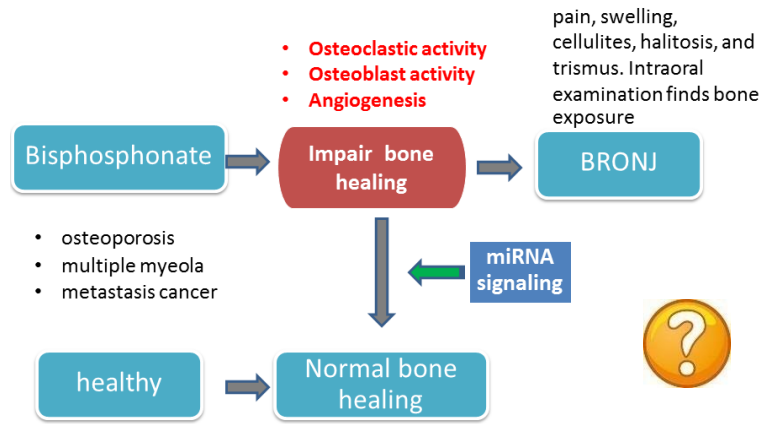
Application and expectation of research

This study will provide knowledge for developing a novel approach for management of incomplete healing extraction socket in MRONJ.

Key words

Bisphosphonates related osteonecrosis of the jaw, microRNA-profiling, angiogenesis, bone remodeling

Conceptual Framework



Chapter II

Literature review

1. MRONJ definition

Patients are distressed from medication-related osteonecrosis of the jaw (MRONJ) such as bisphosphonates (BPs). The symptoms that often has are including pain, swelling, cellulites, halitosis, and trismus. An intraoral examination observes bone exposure at upper or lower jaw, pathologic fracture, oral-cutaneous fistula, or presence of infection. The lesions will occur in the oral cavity for more than 8 weeks with a history of previous bisphosphonate drug used and never exposed to a radiation therapy (Ruggiero et al., 2014).

2. Burden of disease

Patients who suffer from pain, eating discomfort, self-consciousness, unsatisfactory diet, interrupted meals, irritability, have decreased quality of life and emotional status. In addition, the symptoms are more likely to occur depending on the stage of MRONJ (Miksad et al., 2011).

3. Incidence of MRONJ

The incidence of MRONJ varies among many studies depending on a type of disease, method of the study, or epidemiological data. The incidence in osteoporosis patients that were treated with an orally administration of BPs is 1.04–69/100,000 patients per year and treated with an intravenous administration is 0–90/100,000 patients per year. The incidence of MRONJ in the general population, which is 0.001%, is similar to or slightly less than the incidence of MRONJ in patients with osteoporosis treated with oral/intravenous bisphosphonate (0.001 to 0.01%) (Khan et al., 2015). The incidence of MRONJ in cancer patients is higher than MRONJ in osteoporosis patients. The range can be varied from 0.8 to 12% (Kühl et al., 2012).

4. Risk factor of MRONJ

The previous study of MRONJ performed in the 2,400 cases has reported that more than 61% of patients were female. The exposed bone observed in a higher number at the mandible (65%) compared to the maxilla (27%) and 8% were found at both jaws (Filleul et al., 2010). The multivariate analysis showed that smoking, the BPs cumulative dose, steroid intake, maxillary location of lesion, and tooth extraction may significantly pose the risk of having severe stage of MRONJ (Nisi et al., 2015).

5. Bisphosphonates (BPs)

Bisphosphonates (BPs) are widely used for treating several conditions such as osteoporosis, Paget's disease, multiple myeloma, malignant tumor, and bone metastasis of breast or prostate cancer (Drake et al., 2008; Ruggiero et al., 2014; Yoneda et al., 2017). BPs have been used for management of osteoporosis and bone cancer therapy for 40 years (Russell, 2011). The half-life of BPs is ten years (Ganda, 2013). BPs are divided into two categories; nitrogen containing and non-nitrogen containing BP (E Dunford, 2010; Ganda, 2013).

5.1 The benefits of bisphosphonates

Bisphosphonates (BPs) therapy could reduce fracture risk due to decreasing the rate of bone resorption, reducing medical fees, and increase survival rates (McClung et al., 2013). Osteoporosis patients with BPs treatment for more than 1 year could decrease a high risk of fracture and mortality rate in elderly patients (Black et al., 2006). The use of oral and intravenous BPs for more than 3 years was found to be associated with a decrease in mortality rate of up to 28%. In a recent meta-analysis, older patients treated with BPs over 5 years had an adjusted 27% reduction in risk of mortality (Center et al., 2011). On the other hands, the long-term use of BPs, more than 8 years, posed a

higher risk of bone fracture compared to the less than 3-year administration (Drieling et al., 2016).

5.2 Drug administration

Alendronate, risedronate, and ibandronate are allowed to use by the Food and Drug Administration (FDA) for oral administration and recommended for treatment osteoporosis. Alendronic acid and risedronate are prescribed for taking usually one tablet per week. Ibandronic acid is taken once a month in oral route or IV route per three months. Zoledronic acid is subjected to be infused once a year.

The regimens for using BPs for treatment osteoporosis are as followed; Daily ibandronate oral regimen (2.5 mg/day) is better than monthly ibandronate oral regimen (150 mg/month) because of accumulation in skeletal bones (Zaidi et al., 2007). Monthly (150 mg/month) and daily (75 mg /2 consecutive days) risedronate dosing regimens had no difference in benefit of bone turnover suppression and increase bone mass (Delmas et al., 2008a; Delmas et al., 2008b). Zoledronic acid (ZA) (5 mg/year) injection is used for treating patients with menopausal osteoporosis (Black et al., 2007). ZA is also recommended for treatment of malignant tumor and multiple myeloma. ZA therapy is easier to use than pamidronate because it can be administered intravenously only once a year with a short-onset of 30 minutes together with a longer duration of action (Sunyecz, 2008). This administration reduces the need for repeated infusion, cost, and offers a better quality of life. ZA can reduce bone-related disease in breast cancer patients with metastasis into bone and increases survival rate at 5 years from breast cancer (Coleman et al., 2011).

5.3 Mechanism of action

BPs are used for therapy of skeletal disorders caused by excessive or imbalanced skeletal remodeling, because of its high affinity and deposition into bone or other tissues (Filleul et al., 2010). BPs was the first line treatment of osteoporosis and skeletal metastasis because BPs affected osteoclastic /osteoblastic activity and anti-angiogenesis (Ruggiero et al., 2014). BPs inhibited osteoclastic activity, which led to a reduction of osteoblasts activation, consequently decreased bone formation (Ganda, 2013).

BPs, for example; zoledronate, could also have anti-angiogenic activity at 2, 7, 21 days after intravenous administration (Coleman et al., 2011). Angiogenesis is a process of new capillary formation, which is important for wound healing. To promote angiogenesis, blood vessels needed a degradation of basement membrane to permit endothelial cell migration and proliferation into surrounding matrix. Together with the collaboration of proteolytic enzyme (PA) and matrix metalloproteinase (MMP) that could be up-regulated by growth factors induced angiogenesis (Mignatti and Rifkin, 1996). After the catabolism of the basement membrane, endothelial cells promptly moved to the target area and established a proliferation of endothelial cells by the signals from growth factors and cytokines (Liekens et al., 2001). There is a variety of angiogenesis related growth factors, the most essential angiogenic factors are such as vascular endothelial growth factor (VEGF) and fibroblast growth factor-2 (FGF-2).

The vascular endothelial growth factor (VEGF) in blood circulation is a marker of angiogenesis. VEGF is found in various tissues such as brain, kidney, liver, and in several cells (Veikkola and Alitalo, 1999). In vivo study showed that

high VEGF level could stimulate endothelial migration and activation in human surgical wound fluid (Nissen et al., 1998).

ZA could induce a reduction in mRNA expression of VEGF significantly (Santini et al., 2003). BPs caused an efficient decrease of VEGF at 24 hours after infusion. The reduction of VEGF was steady after pamidronate infusion and after ZA infusion at 21 days (Santini et al., 2002). BPs could reduce new blood vessels formation in bone because each remodeling tissue required nutrient via blood circulation (Parfitt, 2000). The reduction of angiogenesis due to an indirect effect of bone remodeling and the role of angiogenesis in MRONJ is still unclear (Somerman and McCauley, 2006).

6. Treatment of MRONJ

Despite of no sign of necrotic bone, patients who have risk of developing MRONJ with the history of using BPs or any anti-angiogenic drugs should be notified for the risks of MRONJ and need to follow up. In case of some symptoms present together with those who have oral diseases such as caries and periodontal disease, these patients are suggested to take medications for control chronic pain and infection with antibiotics. If the signs and symptoms present as having necrotic bone, fistulae, signs of infection, or pathologic fracture at inferior border and ramus of the mandible, maxillary sinus and zygoma in the maxilla, the treatment strategies for these conditions will be an antibacterial mouth rinse prescription, antibiotic and analgesic drug therapies, and surgical debridement or resection. Previous studies advised to treat patients with palliative care, but it was insufficient to recover wound healing (Ruggiero et al., 2014). Alternative therapy may be the way to improve and accelerate the wound healing of MRONJ. The use of plasma rich growth factor (PRGF) has been studied in one human clinical trial for a management of MRONJ in cancer patients. After the

surgical resection of necrotic bone and application of PRGF, the results showed enhancing vascularization, regeneration of osseous and epithelial tissue (Mozzati et al., 2012). The stem cell therapy has been also applied in a rat model with satisfied outcomes (Kaibuchi et al., 2016). However, other non-invasive treatment options for MRONJ are still in search.

7. microRNAs

MicroRNAs (miRNAs) consist of a large family of approximately 21 nucleotide-long RNAs that have been recognized as key post-transcriptional regulators. miRNAs function as controlling the activity of ~50% of all protein coding genes and involve in regulating every cellular process. The regulation via miRNAs can be switching-off or modifying the expression of target genes that in turn associates with several human pathologies (Krol et al., 2010).

7.1 Role of miRNAs in the pathogenesis of MRONJ

In searching of the research evidences, the specific miRNAs that target to the pathogenesis of MRONJ have not yet been identified. However, the candidate specific miRNAs associated with MRONJ could be hypothesized according to the mechanism of action of BPs that impacts the angiogenic activity and bone remodeling process after being administered. The miRNAs function associated with both pro-/ anti-angiogenesis, osteoblastic and osteoclastic activity would be presumably play an important role in the pathogenesis of MRONJ.

7.1.1 Angiogenesis-regulatory miRNAs

miRNAs involved in regulation of angiogenic activity, particularly via endothelial function, can be categorized into the pro-angiogenic miRNAs (promote angiogenesis) and the anti-angiogenic miRNAs (inhibit angiogenesis).

Wu et al. summarized the miRNAs associated with angiogenesis as shown in Table 1 and Figure 1 (Wu et al., 2009).

Table 1. Angiogenesis-regulatory miRNAs and their targets (Wu et al., 2009).

microRNA	Biological function	Targets
<i>Pro-angiogenic</i>		
miR-126	Maintain vascular development, regeneration, and integrity	Spred-1, PIK3R2/p85- β , VCAM-1
miR-17-92 cluster	Promote tumor angiogenesis	TSP-1, CTGF, TIMP-1, HIF-1 α ?
Let-7b,f	Regulate sprout formation	Let-7b-TIMP-1; Let-7f-TSP-1?
miR-130a	Regulate angiogenic phenotype of EC	Homeobox gene: GAX, HOXA5
miR-210	Promote EC migration and capillary-like structure formation	Ephrin-A3, HIF-1 α
miR-378	Promote tumor angiogenesis	SuFu, Fus-1
miR-296	Promote EC migration and tube formation, and tumor angiogenesis in vivo.	HGS
<i>Anti-angiogenic</i>		
miR-221/miR-222	Inhibit EC migration, proliferation	c-kit, eNOS
miR-328	Reduce formation of capillary structure	CD44
miR-15b/miR-16	Induce cell apoptosis	VEGF, Bcl-2?
miR-20a/ miR-20b		VEGF

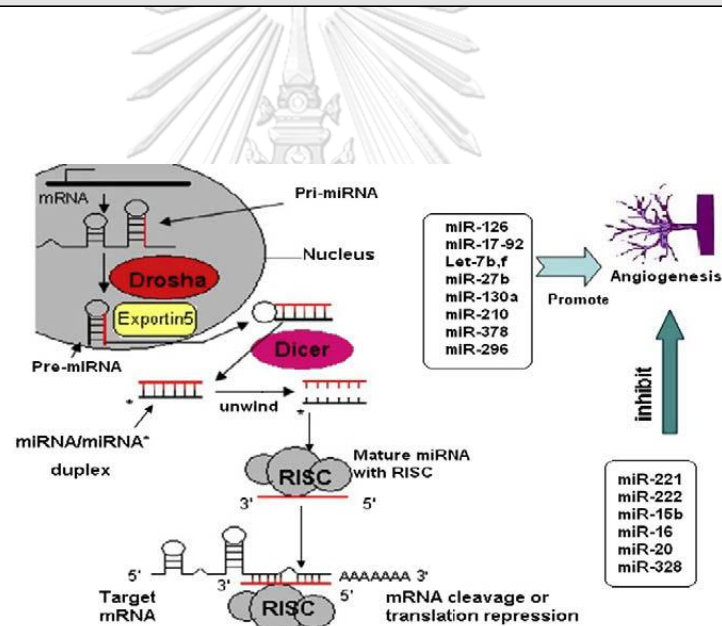


Figure 1 Biogenesis of angiogenesis-related miRNAs (Wu et al., 2009).

(1) Pro-angiogenic microRNAs

● miR-126

miR-126 is a short non-coding RNA molecule that regulated the expression in endothelial cells. It locates in chromosome 9q34.3 which encoding for epidermal growth factor like-7 (Egfl7) that was expressed only in high-grade peripheral vascular

endothelial cells (Bartel, 2004; Wu et al., 2009). miRNAs could bind directly to DNA, prevented transcription or translation of mRNA and promoted degradation of mRNA. The majority targets of the miRNA-126 was the EGFL7 host gene (Parker et al., 2004).

EGFL7 controls cell migration and vessels formation in normal organs, whereas, higher EGFL7 level could promote angiogenesis that further supplied the nutrient for cancer cells and accelerated tumor cells growth. An animal model showed the loss of vascular integrity and hemorrhage in embryonic zebra fish due to an inhibition of miR-126 (Fish et al., 2008). The miR-126 knocked-out mice demonstrated delayed vessel formation, bleeding and mortality during embryos (Kuhnert et al., 2008).

miR-126 also controlled defection of VEGF and other growth factors by decreased PI3 kinase activity that was necessary to VEGF production by reducing miRNA production (Wang et al., 2008).

- **miR-17~92 cluster**

The miR-17~92 cluster was discovered as tumor promoting miRNA. This gene cluster encodes miR-17, miR-18, miR-19a, 20a, miR-19b-1 and miR-92-1. miR-17~92 has been shown to regulate c-Myc to induce B cell lymphoma in mice (He et al., 2005). The upregulation of miR-17~92 promoted tumor angiogenesis and increased Ras protein level *in vivo*. *In vitro*, the downregulation of miR-17~92 reduced endothelial cell sprouting and tube formation (Suárez et al., 2008).

Angiogenesis process was occurred by which miR-17~92 inducing target anti-angiogenic proteins such as thrombospondin-1 (Tsp1) and connective tissue growth factor (CTGF). The absence of miR-17~92 in mice resulted in dysfunction of lung and defect in ventricular septum that finally led to the immature growth and death since an early post-natal stage (Ventura et al., 2008).

- miR-720

Previous study investigated blood test screening for early detected colorectal malignancy. miR-720 was significantly high in patient with colorectal cancer (CRC). Whereas after treatment with surgical procedure, miR-720 in serum significantly was more decreased than healthy patient (Nonaka et al., 2015). Other finding found the miR-720 repression in coronary artery disease treated with vessel therapy by infrared that effect to vasohibin1 (VASH1) that was a dominant process in anti-angiogenesis. Wang et al. demonstrated pathway that promote endothelial cell activity in Figure 2 (Wang et al., 2014). Infrared treatment directly induced miR31 inhibition of both TBXA2R and FAT4 pathway. miR-720 was restrained via FAT4 suppression. This act miR-720 inhibited VASH1 resulted in promote-endothelial progenitor cell (EPC) migration and blood vessel formation. Further study showed miR-720 over-expression in Breast cancer. Abundant of disintegrin and metalloproteinase 8 (ADAM8) serum level were found in cancer patient. miR-720 was controlled by ADAM8 via ERK pathway signal, β 1-integrin and VEGF-A that facilitated tumor invasion and blood vessel formation (Das et al., 2016).

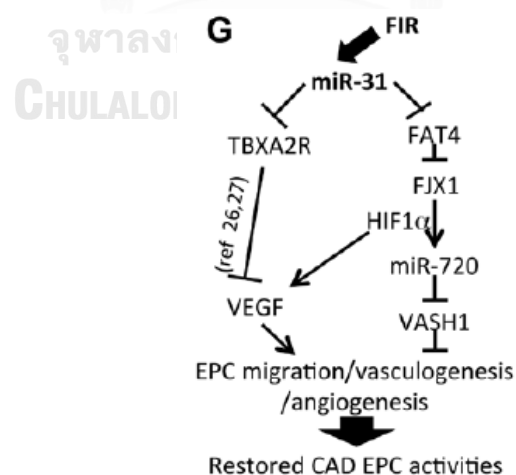


Figure 2 miR-720 pathway that promote endothelial cell activity (Wang et al., 2014).

- miR-378

miR-378 has been demonstrated as having an angiogenesis capacity *in vivo*. The binding sites of miR-378 locate in the VEGF 3'-UTR (Hua et al., 2006). This miRNA acted as anti-apoptosis and overexpressed in cancer cell lines. miR-378 enhanced angiogenesis by means of repressing the expression of two tumor suppressors, Sufu (suppressor of fused) and Fus-1 (tumor suppressor candidate 2, TUSC2) (Lee et al., 2007). This result induced VEGF and angiopoietin expression. The injection of miR-378 led to cancerous cell line (Wang and Olson, 2009). Moreover, downregulation of MiR-378 had a synergistic effect with angiotensin-II that induced severe cardiac hypertrophy, fibrosis, and cardiac dysfunction in Mice (Nagalingam et al., 2014). miR-378 is one of the miRNAs that regulate angiogenesis targeting on the non-endothelial cell. The Figure 3 illustrated the signaling pathway in controlling angiogenesis via miRNAs targeting on non-endothelial cell (Wang and Olson, 2009).

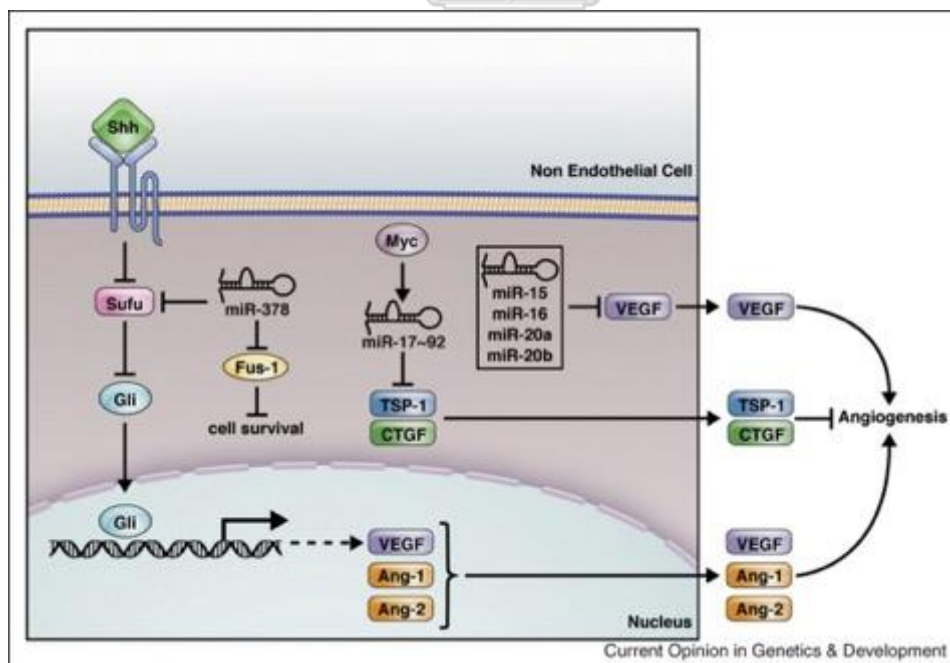


Figure 3 Target protein of miRNA in non-endothelial cell. (Wang and Olson, 2009).

- **miR-296**

miR-296 belongs to the family of “angiomirs” in endothelial cells, which increased levels of pro-angiogenic growth factor receptors such as VEGF receptor (VEGFR) and platelet-derived growth factor receptor (PDGFR). Furthermore, VEGF was also able to increase miR-296 level in order to control balance of blood remodeling in endothelial cells or glioma cells. Meanwhile, miR-296 expression affected on hepatocyte growth factor-regulated tyrosine kinase substrate (HGS) which resulted in an increase of VEGFR2 and PDGFR- β protein levels in a “feedback loop” manner. This cross-talk mechanism controlled miR-296 levels and angiogenic growth factor together. (Würdinger et al., 2008)

- **miR-210**

miR-210 stimulated VEGF affecting cell migration, cell growth, and blood vessel formation. *In vitro*, especially in low oxygen condition, miR-210 targeted at hypoxia – inducible factor 1 alpha (HIF 1 α) and ephrin-A3. HIF 1 α could promote angiogenesis via tyrosine kinase 3 receptor (Fasanaro et al., 2008; Pulkkinen et al., 2008). In rodent, miR-210 stimulation caused heart failure cardiac myocyte and cerebral artery blockade (Jeyaseelan et al., 2008; Tatsuguchi et al., 2007). Tuning by miR-210, erythropoietin-producing human hepatocellular receptors (Ephs) and ephrin A3 molecules regulated the remodeling of blood vessels and played essential roles in endothelial cells such as chemotaxis and forming capillary tube (Kuijper et al., 2007)

(2) *Anti-angiogenic microRNAs*

- **miR-221/miR-222**

miR-221 and miR-222 locate side by side on Xp11.3 chromosome, suggesting their coordinated regulatory role. *In vitro*, miR-221 inhibited endothelial cell migration,

proliferation, and angiogenesis via targeting stem cell factor (SCF) receptor called “c-Kit”. In human umbilical vein endothelial cells (HUVECs), SCF enhances survival, migration, and capillary tube formation in a dose-dependent manner. miR-221/miR-222 are responsive to high glucose concentration (Altuvia et al., 2005; Polisenio et al., 2006). In vivo experiment has demonstrated that HUVECs treated with high concentration of glucose induced miR-221 expression which consequently halted endothelial cell migration and reduced c-Kit expression. In contrast, the application of the antisense miR-221 oligonucleotide in turn reduced the expression of miR-221 and restored c-Kit expression in HUVECs. Therefore, miR-221-c-Kit pathway is suggested to play a crucial role in diabetes associated vascular dysfunction and impaired wound healing (Li et al., 2009).

Furthermore, an indirect effect from stimulated miR-221 also induced protein level of endothelial nitric oxide synthase (eNOS) that provoked multiple regulations, including vascular tone, cellular proliferation, leukocyte adhesion, and platelet aggregation (Förstermann and Münzel, 2006). Figure 4 demonstrated the miRNAs involve in regulating gene expression targeted on angiogenesis via endothelial cells.

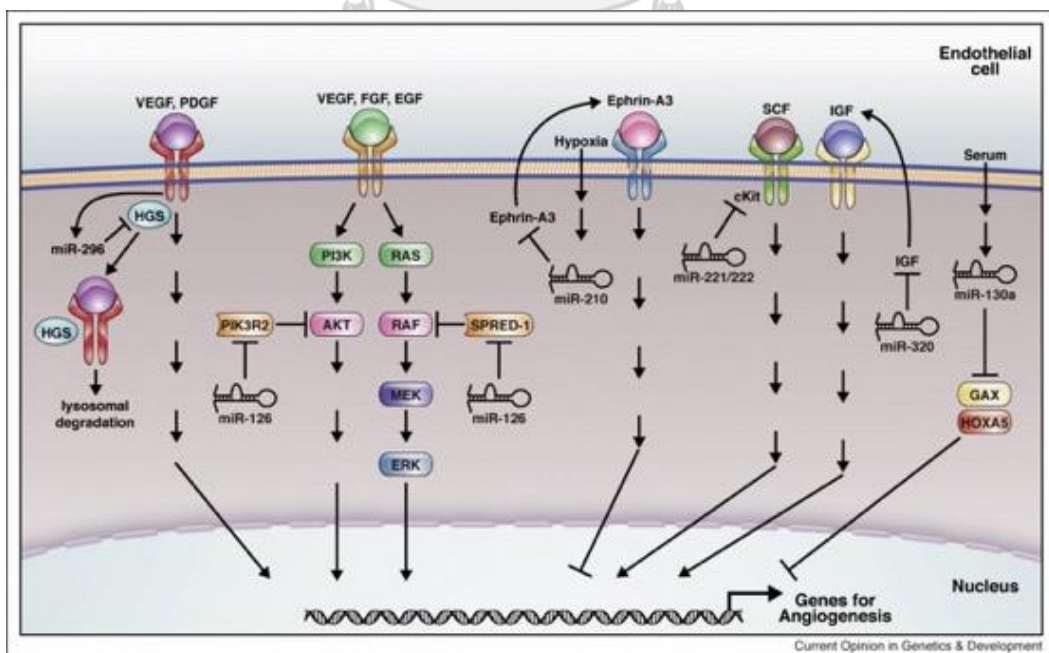


Figure 4 Target protein of miRNAs in endothelial cell (Wang and Olson, 2009).

- **miR-663**

miR-663 has been a cancer suppressor gene that could regulate tumor progression and associated with heart diseases. Previous study found overexpression of miR-663 in human umbilical vein endothelial cells (HUVECs). miR-663 accumulation induced endothelial cells alteration. In high uric concentration, vessel migration was inhibited by overexpression of miR-663 via repressing Transforming Growth Factor-b1 (TGF-b1) resulted in anti-angiogenic effect (Hong et al., 2015). miR-663 used as a biomarker in neoplastic formation by targeting JUNB, MYH9 in Vascular smooth muscle cells (VSMCs) (Michaille et al., 2018). Stimulation of blood vessel formation by platelet-derived growth factor (PDGF) could induced lower miR-663. miR-663 from adenovirus transfection in smooth muscle endothelial cell dramatically decreased PDGF then a number of vascular formation were inhibited (Li et al., 2013). Nevertheless, some study reported opposite outcome of promoting angiogenic activity. Other reseaches attempted to limit miR-663a expression that led to down regulation of VEGF in endothelial cell. On the other hand, miR-663a induced Activating Transcription Factor 4 (ATF4) and VEGF pathway in hyperlipidemic condition (Afonyushkin et al., 2012).

- **miR-652 -3p จุฬาลงกรณ์มหาวิทยาลัย**

In vivo study found overexpression of miR-652 in carotid tissue and cholesterol plaques. Moreover, inhibition of miR-652 – 3p utilized endothelial cell proliferation in carotid artery. After arterial damages, high level of miR652 was dramatically detected in dyslipidemic patient via promoting CyclinD2 expression resulted in blood vessel repair (Huang et al., 2019).

7.1.2 Bone remodeling-regulatory miRNAs

(1) Promote osteoblastic activity

- **miR-34**

miR-34 has been demonstrated as having osteogenesis activity *in vivo* study. Over expression of miR34a was found in irradiation inducing osteogenesis rat model. miR-34a inhibited newly formed bone in tibial bony defect by repressing NOTCH 1 that control cell determination (Liu et al., 2019). The interaction of NOTCH1 and miR-34 were shown in previous study that investigated miR-34 in Human Adipose-Derived Stem Cells (hASCs). Up regulation of miR-34 by transfection in lentivirus inhibited 3 genes such as Retinol-Binding Protein 2 (RBP2), CYCLIN D1 and NOTCH 1 influenced on suppressed the protein levels of RUNX and P27 facilitated osteoblastic activity. Figure 5 illustrated the RBP2/NOTCH1/CYCLIN D1 signaling pathway in controlling osteoblastic activity (Fan et al., 2016). Other investigation found miR-34 inhibited identified transforming growth factor β -induced factor 2 (TGIF2) led to prevention of osteoporosis and bone resorption. TGIF2 suppression reduced osteoclastogenesis and blocked anti-osteoclastic activity (Krzyszinski et al., 2014).

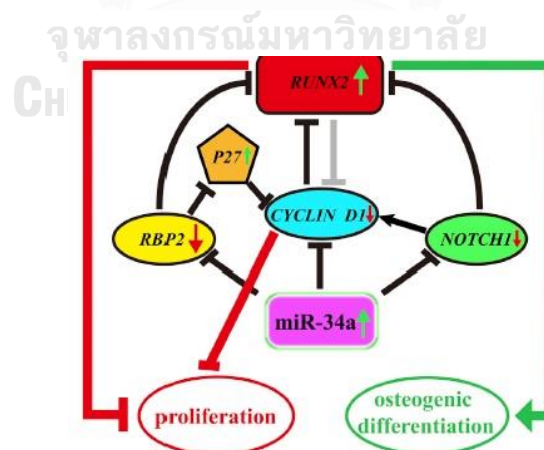


Figure 5 RBP2/NOTCH1/CYCLIN D1 collaboration in osteogenic activity (Fan et al., 2016).

miR-34a regulated silent information regulator 1 (SIRT1) expression. The inhibition of SIRT1 led to an increase in acetylated p53 controlling cell cycle and apoptosis. miR-34 act as tumor suppressor gene by interfering SIRT1 that necessary in angiogenic process. This research that investigated the connection between miR-34 and SIRT showed high level of miR-34 inhibited the SIRT expression consequently, endothelial cell proliferation was decreased. In the same vein, stimulated SIRT led to downregulation of miR-34. Moreover, some study claimed that miR-34 has been one of aging cell indicator (Ito et al., 2010).

(2) *Inhibit osteoblastic activity*

- **The miR-23a~27a~24-2 cluster**

Runx-related transcription factor 2 (RUNX2) is a protein that is encoded by the *RUNX2* gene in humans. The function of this protein is to promote osteoblast growth via cell cycle regulation. Runx2 is considered as a crucial transcription factor for osteoblastogenesis (Lian et al., 2012).

The miR-23a~27a~24-2 cluster is one of 11 miRNAs that has been identified as negative tuning of Runx2 and SATB2 in mesenchymal cells, which suppressed osteoblast maturation (Zhang et al., 2011).

(3) *Promote osteoclastic activity*

- **miR-21**

miR-21 could regulate osteoclastogenesis by promoting osteoclast differentiation in mice bone skull. The upregulation of miR-21 expression level found to increase the number of osteoclasts (Zhou et al., 2012). RANKL/OPG ratio has a significant role in bone homeostasis. The downregulation of miR-21 increased OPG level resulting in increasing bone formation (Pitari et al., 2015). MiR-21 also stimulated bone resorption process by inhibited PDCD4, which blocked cFOS function which is a AP-1 transcription

factor complex, resulted in the promotion of functional osteoclast in mouse (Wagner, 2010).

- **miR-31**

miR-31 targets on Ras homolog gene family, member A (RhoA) which subsequently stimulates osteoclast maturation. The induction of miR-31 established cytoskeleton arrangement in a present of actin ring that led multinucleated cells to attach onto the mineralized matrix (Mizoguchi et al., 2013).

- **miR-223**

miR-223 is mostly found in hematopoietic cell lineages. The target of miRNA-223 is the transcriptional repressor Nuclear Factor IA (NFI-A) which promotes an expression of the CSFR1/M-CSFR receptor collaborated by PU.1 (purine-rich binding protein 1). This subsequently suppressed differentiation into osteoclasts in osteoclast precursor. While, the loss of this repressor permitted transcriptional activation of the macrophage colony-stimulating factor receptor (M-CSFR) gene (Sugatani and Hruska, 2007). *In vitro*, the upregulation of miR-223 inhibited osteoclast differentiation by reducing TRAP+, which resulted in the absence of osteoclast cells formation (Sugatani and Hruska, 2007). However, miR-223 could be repressed when treating osteoclast precursor with TNF- α and RANKL in RAW264.7 cells (Kagiya and Nakamura, 2013). Table 2 summarized the miRNAs and their roles that might associate with the pathogenesis of MRONJ in terms of both angiogenesis and bone remodeling.

Table 2. miRNAs and their targets involved in the pathogenesis of MRONJ in review literature.

miRNA	Species	Target gene	Endogenous miRNA expression	miRNA function	Ref.
miR 126 (+)	Mice, zebra fish	Spred-1, PIK3R2/p85- β , VCAM-1	Increase EGFL7, VEGF	Repressing vascular cell adhesion molecule-1 (VCAM- 1)	Kuhnert et al., 2008. Fish et al., 2008.
miR-17~92 (+)	Mice	TSP-1, CTGF, TIMP-1, HIF-1 α , c-myc	Increase Ras VEGF	-Promote tumor angiogenesis -B cell lymphoma -EC sprout and tube formation	He et al., 2005 Ventura et al., 2008.
miR-378 (+)	Mice	SuFu, Fus-1	Increase CD34 ⁺ proge- nitor cells, VEGF, angiopoietin	Promote tumor angiogenesis	Hua et al., 2006. Wang and Olson, 2009.
miR-296 (+)	Human	HGS	Increase VEGFR2 and PDGFR- β	Promote EC migration, tube formation and angiogenesis	Würdinger et al., 2008.

miRNA	Species	Target gene	Endogenous miRNA expression	miRNA function	Ref.
miR-210 (+)	<i>In vitro</i> , mice	HIF, ephrin-A3	Increase VEGF	cell migration, cell growth and form blood vessel	Kuijper et al., 2007. Tatsuguchi et al., 2007.
miR-34 (+)	<i>In vivo</i> rat	CYCLIN D1 and NOTCH 1	Increase RUNX2	Increase osteoblastic activity osteoclastogenesis	Liu et al., 2019 Fan et al., 2016
miR-720 (+)	Human	VASH1 ADAM8	Increase VEGF	MC migration, vasculogenesis, angiogenesis	Wang et al, 2014 Das et al, 2016
miR652-3p (-)	<i>In vivo</i>		Cyclin-D2	Inhibit EC proliferation	Haug et al, 2019

miRNA	Species	Target gene	Endogenous miRNA expression	miRNA function	Ref.
miR-663 (+)(-)	Human	JUNB, MYH9 ATF4	TGF- β 1 Increase VEGF	Inhibit EC migration Promote EC repair	Li et al, 2013 Afonyushkin et al, 2012
miR-221 (-)	<i>In vitro</i>	c-kit, eNOS	Activated proliferation and anti-apoptosis	Inhibit EC migration and proliferation	Altuvia et al., 2005. Förstermann and Münzel, 2006.
miR – 302a3p (+)	In vitro	TGF- β , BMP, COUP-TFII, PGE-2	Upregulate RANKL	Promote osteoclast differentiation	(Irwandi, 2015)
miR-23a~27a~24-2 (-)	mouse	SatB2, Runx2, Hoxa10	Repress expansion and lineage direction and limit bone mass	Interrupted osteoblast differentiation	(Zhang et al., 2011)
miR-204 (-)	mouse	Runx2	Repress expansion and lineage	Interrupted osteoblast differentiation	(Hassan et al., 2010) (Zhang et al., 2011)
miR-31 (+)	Mice	RhoA	Upregulate RANKL	Multinucleated cells attach to the mineralized matrix	Mizoguchi et al., 2013

miRNA	Species	Target gene	Endogenous miRNA expression	miRNA function	Ref.
miR-223 (-)	<i>In vitro</i>	NFI-A	CSFR1/M-CSFR, PU.1	Inhibit osteoclast differentiation	Sugatani and Hruska, 2007 Kagiya and Nakamura, 2013

* (+) promote, (-) inhibit, EC = endothelial cell

Therefore, the aim of this study is to investigate microRNA profiles associated with angiogenesis and bone remodeling that have an effect on bone healing of the extraction socket in Medication-related osteonecrosis of the jaw in a rat model.



Chapter III

Research and methodology

The animal experiment

The animal protocol was improved by Chulalongkorn University Animal Care and Use Committee (Ethic no.1973005). Sprague Dawley (SD) rats (6-week-old), weight range (195-205 g) were kept in a laboratory environment for 2 weeks and randomly divided into 2 groups;

Group 1 (n = 10): administration of zoledronate (66 μ g/kg; Zometa, Novartis Pharma, Stein AG, Stein, Switzerland) and dexamethasone (5 mg/kg; Dexton, T.P. Drug Laboratory, Bangkok, Thailand).

Group 2 (n = 7): administration of normal saline solution (Klean&Kare, Bangkok, Thailand) as a control group

Each drug was injected intraperitoneally into SD rats on Monday, Wednesday, and Friday for 4 weeks. Two weeks after the first administration (day 0), the maxillary right and left first molars were extracted under general anesthesia by intraperitoneal injection of tiletamine-zolazepam (Zoletil; 40 mg/kg) and xylazine (2 mg/kg). Then, animals were sacrificed on day 0, 14, and 28 after extraction, and the upper jaw was collected. The photographs of maxilla were taken in each group. Then, the maxillary tissues were dissected and removed. The samples of maxilla were separated into 2 halves antero-posteriorly. The first half was used as the bone sample for microRNA analysis. Another half of maxilla was fixed in 10% formalin for further micro-CT and histological analysis. The experimental diagram, drug administration and timeline of experiment were shown in Figure 6.

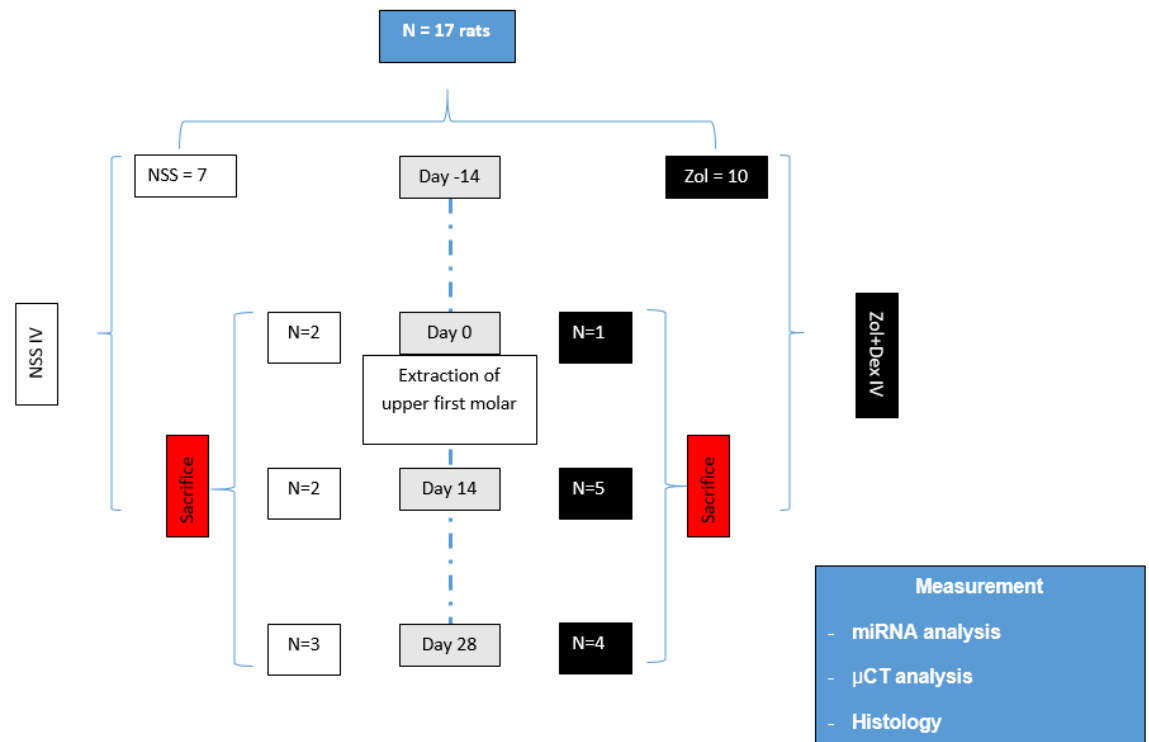


Figure 6 Experimental diagram and timeline.

Body weight evaluation

Bodyweight of rats were measured at baseline, day 7 after drug administration, day 0 of tooth extraction, day 7, 14 and 28 after tooth extraction.

Gross and radiographic evaluation

In the test group, a presence of MRONJ was confirmed by visual inspection and radiographic analysis on the epithelial closure, bone exposure and new bone formation after 4 weeks of tooth extraction (Zandi et al., 2016).

Micro-CT analysis

New bone formation in the extraction sockets was visualized using a micro-computed tomography (CT) system (SCANCO Medical, Brüttisellen, Switzerland) at the Mineralized Tissue Research Unit, Faculty of Dentistry, Chulalongkorn University. The maxillary bones were scanned using micro-CT with an X-ray source of 70 kV/113 μ A with a slice thickness of 15 μ m.

To assess new bone formation, a region of interest (ROI) was established in a micro-CT image. The axial view was used to identify the interproximal crestal bone between the upper second molar and the extraction socket. The micro-CT slice which represented the distance of 0.5 mm apical to the first identifiable alveolar crest was selected as the slice of interest. Then, the ROI was created by making the square with the size of 0.5 x 0.5 mm² at the center of an extraction socket on this slice (Figure 7A). In order to determine bone volume in the extraction socket, the volume of interest (VOI) of 0.5 x 0.5 x 0.5 mm³ per extraction socket was established by using the ROI as a reference (Figure 7B). Bone volumes and gross 3D images were processed and compared among groups using ImageJ software (Fiji, NIH, USA) and 3D viewer (Microsoft, USA).

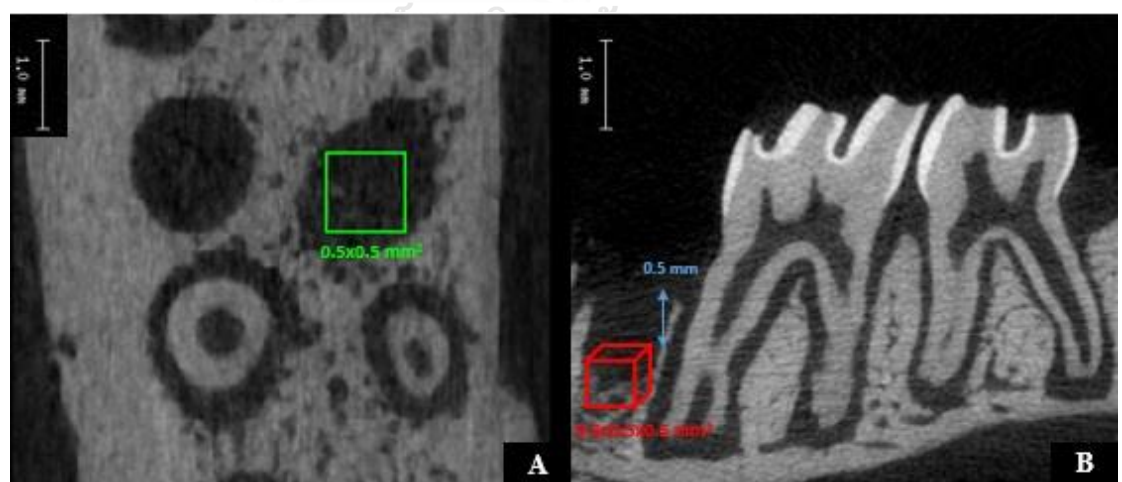


Figure 7 Setting of the region of interest (ROI) and volume of interest (VOI) in an extraction socket

Histological analysis

The new bone formation was examined on day 0, 14, and 28 after extraction. The maxillary tissues were removed, fixed in 10% formalin, the tissue samples were decalcified with 0.1mol/l EDTA and embedded in paraffin. Then, the section was cut in a longitudinal section in 5-mm thickness using a microtome and was stained with the hematoxylin and eosin (H&E). Histological analysis was determined at the magnification of 1X by making the square with the size of 0.5 x 0.5 mm² covered the new bone formation which distance from furcation of upper maxillary first molar was 2 mm. At the magnification of 8X, a number of osteocyte, immature osteocyte and empty osteocyte in lacunae were counted by using Photoshop CC (Adobe systems Incorporated, California, U.S.A).

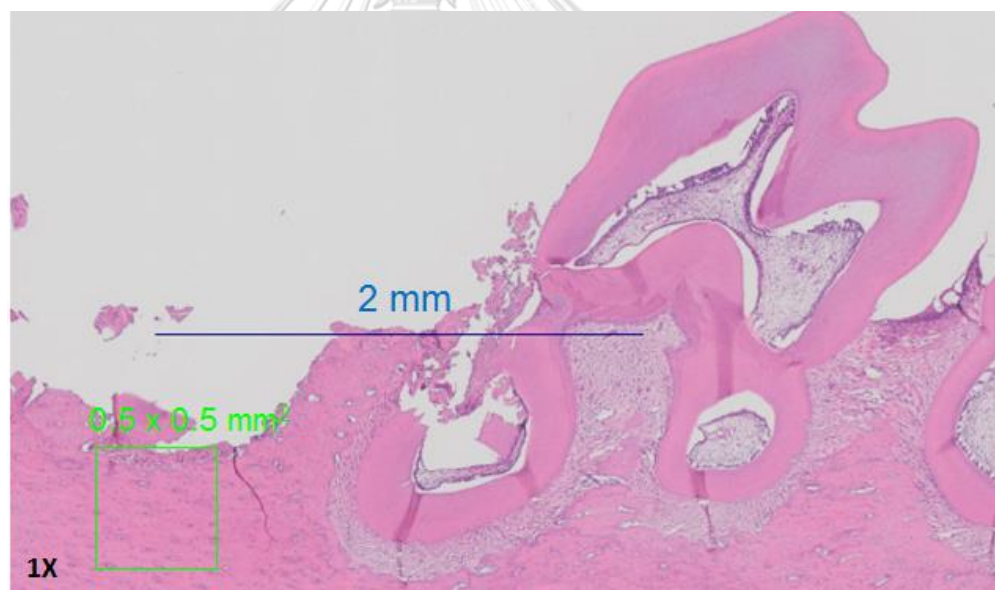


Figure 8 Setting of the region of interest (ROI) for histological analysis in extraction socket.

miRNA analysis

RNA isolation, reverse transcription (RT) and quantitative polymerase chain reaction (qPCR)

The bone sample was collected from an extraction socket with a 2 mm-diameter trephine bur and then kept in RNAlater (Qiagen, Valencia, CA,USA). The bone tissue was homogenized by metal beads (size 2.38 mm; Qiagen, Valencia, CA,USA) with

a homogenizer machine (Powerlyzer™ 24; Qiagen, Valencia, CA, USA) for 3 minutes. Total miRNAs were extracted by miRasy mini kit (Qiagen, Valencia, CA, USA). The amount of RNA was determined at an absorption of 260/280 nm using a micro-Volume UV-Vis Spectrophotometer for Nucleic Acid and Protein Quantification (NanoDrop2000, Thermo Scientific).

For miRNA, 1 µg of each RNA sample was converted to cDNA by using miScript II RT Kit (Qiagen, Hilden, Germany) on thermal cycler, and the real time PCR was performed using Quantitect SYBR Green PCR mastermix (Qiagen, Hilden, Germany) on PCR detection system (MiniOpticon quantitative PCR, Bio-Rad, Hercules, CA). The candidate microRNAs that our study investigated are shown in Table 3. Customized primers were designed and supplied by GeneGlobe (Qiagen, Valencia, CA, USA) in customized 96-well plate qPCR array. The list of primers is shown in Table 4. The PCR conditions were 95°C for 15 min followed by 40 cycles of amplification consisting of 94°C for 15 sec, 55°C for 30 sec, and 70°C for 30 sec. All samples were run in duplicates, and results were averaged for gene expression analysis. Raw quantification cycle values (Ct) were collected. The Ct values > 35 were considered to be excluded. Each value of miRNA were normalized by RNU6-2 (Qiagen, Valencia, CA, USA) using $2^{-\Delta\Delta Ct}$ method.

Statistical analysis

All data was presented as the mean ± standard error and analyzed with SPSS 22.0 statistic software. The independent t-test was performed to evaluate the differences in relative expression of candidate miRNAs, to compared quantity of new bone formation from µCT scan and the differences in number of empty osteocyte in lacunae at 28 days after tooth extraction. The *p-value* of < 0.05 was considered as significance.

According to the above review literatures, financial and COVID-19 situation, the number of studied miRNAs was reduced. The list of candidate miRNAs involved angiogenic process and bone remodeling that were used in this study were demonstrated in Table3.

Table 3. List of candidate miRNAs in MRONJ rat model.

Mechanism	miRNAs	Target gene	Reference
Promote – angiogenic activity	miR-720	VASH1	Wang et al., 2014
	miR-663	ATF4	Afonyushkin et al, 2012
Anti - angiogenic activity	miR-34a-5p	SIRT1	Lian et al., 2012
	miR-652-3p	Cyclin D2	Huang et al., 2019
	miR-663	TGF- β 1	Hong et al., 2015
		JUNB, MYH9	Michaille et al., 2018
Promote - osteoblastic activity	miR-34a-5p	Cyclin D1, NOTCH1	Fan et al., 2016
Inhibit - osteoblastic activity	miR-23a-3p	RUNX2	Hassan et al., 2010
	miR-23b-3p	RUNX2	Guo et al., 2016
	miR-27a-3p	HOXA10, RUNX2	Lian et al., 2012
		RUNX2, Tcf-1	Zhao et al., 2015
	miR-24-3p		
Inhibit – osteoclastic activity	miR-34a-5p	Tgif2	Jing et al., 2015

Table 4. Designed primer of candidate miRNAs.

miRBase Accession No.	Mature miRNA ID	miScript Primer Assay Catalog
MIMAT0000255	hsa-miR-34a-5p	MS00003318
MIMAT0003322	hsa-miR-652-3p	MS00010451
MIMAT0003326	hsa-miR-663a	MS00037247
MIMAT0005954	hsa-miR-720	MS00014833
MIMAT0000078	hsa-miR-23a-3p	MS00031633
MIMAT0000418	hsa-miR-23b-3p	MS00031647
MIMAT0000084	hsa-miR-27a-3p	MS00003241
MIMAT0000080	hsa-miR-24-3p	MS00006552



Chapter IV

Results

Animal model

From total animal samples (N = 19), there was two rats died during the course of experiment. In Zol group, one rat was died during the blood collection procedure due to the heart attack. Another rat from NSS group was died immediately after tooth extraction due to overdosage of anesthetic drug and nephrotoxicity. Therefore, at the end point of this study, there were 17 rats remaining in this study, resulting in an inadequate number of study sample. Accordingly, the descriptive analysis of the results could be performed.

Changes in body weight

In this study, the body weight was measured only 10 rats. At the baseline, the total mean body weight of 10 rats was 155.0 g. The total mean body weights of rats at 1, 2 and 4 weeks (Day 7, 14, 28) after tooth extraction were 201.25 g and 207.19 g and 243.38 g respectively. Body weight in NSS group was greater than Zol group at all time points. On the day of operation (Day0), body weight in Zol group was lower than NSS group (182.69 g and 225.8 g). Day 7 after tooth extraction, the mean body weight in Zol-treated group was slightly decreased than day 0. Furthermore, after 4 weeks of tooth extraction, the weight difference in the Zol group was similar to the weight difference in Nss group compared to the day of tooth extraction (53.19 g, 54.7 g, respectively) (Figure9).

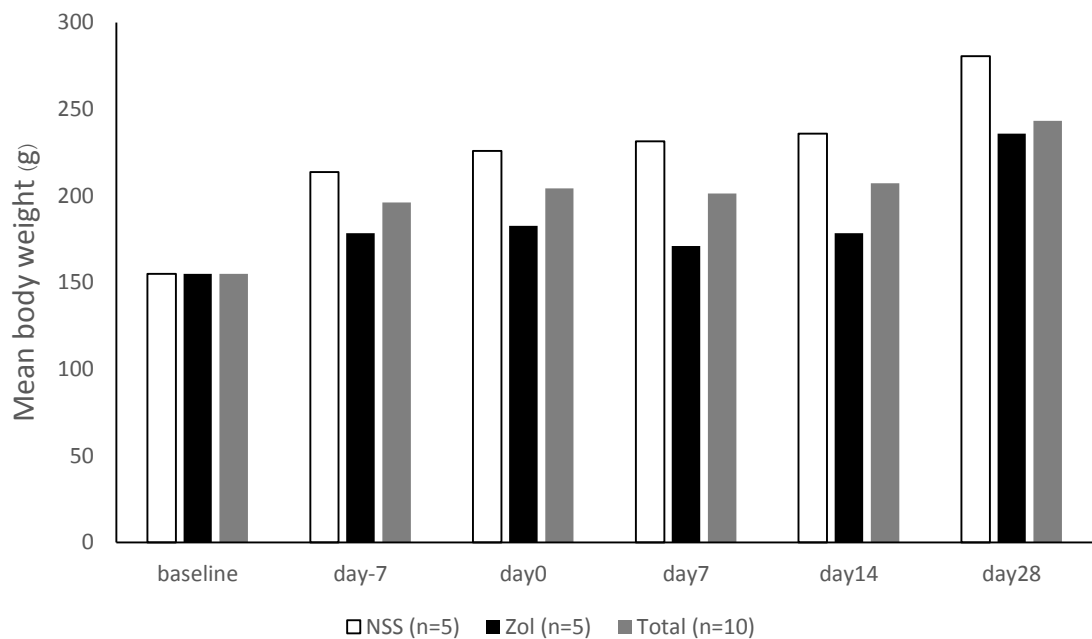


Figure 9 Change in mean body weight at baseline, Day (-7), 0, 7, 14, and 28 of tooth extraction; normal saline administration (NSS), zoledronate and dexamethasone administration (Zol), and total (n=10).

Gross and radiographic evaluation

Two and four weeks after tooth extraction, the extraction sockets in NSS groups (N=4/5) showed normal wound healing, (N=1/5) showed non-coverage and delay wound healing (Figure 10A and 10B). In contrast, brownish color sockets and bone exposure in which indicated the MRONJ appearance were observed in all rats belonged to Zol group (N=9/9) (Figure 10C and 10D). Radiographic finding showed normal bone healing in NSS group (Figure 11A and 11B) and delayed bone healing in the extraction sockets of Zol group (Figure 11C and 11D), 14 and 28 days after extraction. The percentage of bone exposure in both groups 14 and 28 days after extraction is shown in Figure 12.

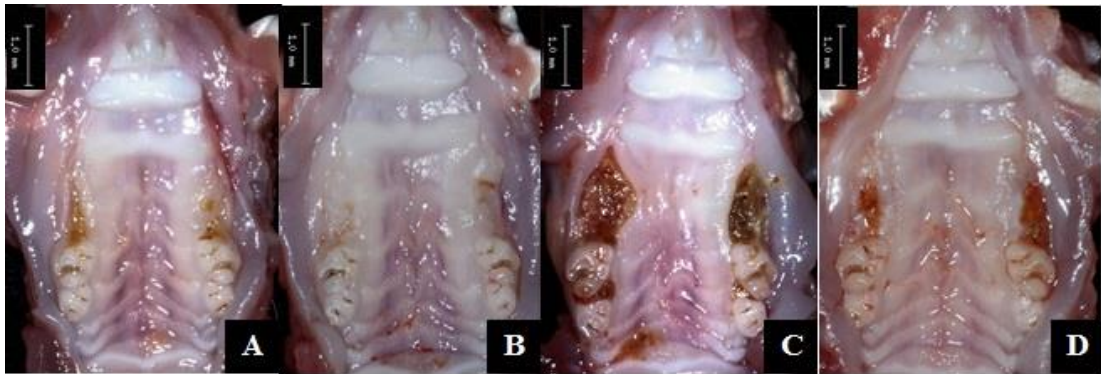


Figure 10 Gross evaluation: 14 and 28 days after extraction, (A) normal saline (NSS) group at day 14, (B) NSS group at day 28, (C) zoledronate and dexamethasone administration (Zol) group at day 14, and (D) Zol group at day 28.

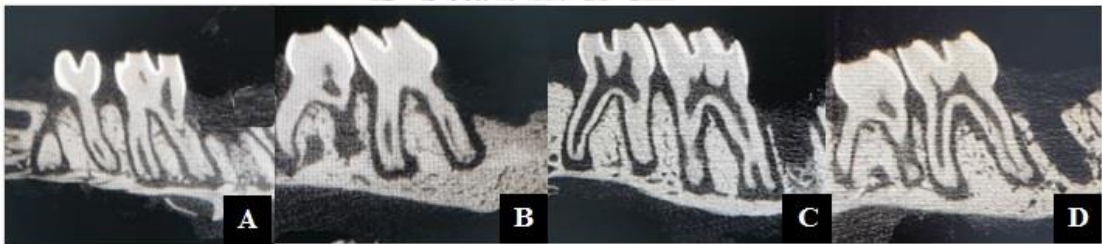


Figure 11 Micro-CT views: 14 and 28 days after extraction, (A) normal bone healing in NSS group at day 14, (B) normal bone healing in NSS group at day 28, (C) showed delayed bone healing in the extraction sockets of Zol group at day 14, (D) showed delayed bone healing in the extraction sockets of Zol group at day 28.

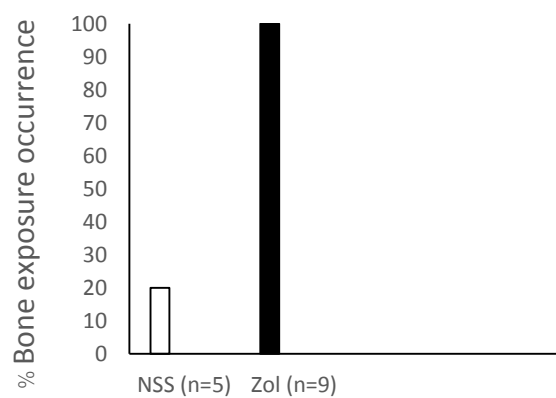


Figure 12 % Bone exposure occurrence (N= 14) : 14 and 28 days after extraction.

Micro-CT analysis

Micro-CT analysis revealed delayed bone formation and irregular trabeculae bone arrangement in the extraction sockets of the Zol group while normal bone formation and trabeculae bone forming were observed in NSS group. The rendering 3D characteristic of bone formation comparing among NSS and Zol group at Day 28 was performed and demonstrated in Figure 13. The lowest amount of calcification was seen in Zol-28 group. Calcification volume was quantified at Day 28 after tooth extraction. Bone volume of newly formed bone in VOI were 0.0764 mm^3 (SE 0.0070 mm^3) in NSS-28 group. In the group of rats that were treated with zoledronic acid, after 28 days of extraction (Zol-28) the bone volume of 0.0342 mm^3 (SE 0.0090 mm^3) was observed. There was a significant decrease in newly formed bone in Zol-28 group compared to the NSS-28 group ($p=0.004$) (Figure 14).

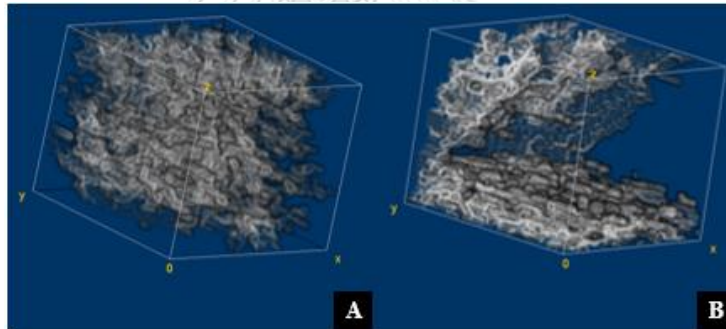


Figure 13 μ CT imaging demonstrated three-dimensional (3D) of volume of interest (VOI) size $0.5 \times 0.5 \times 0.5 \text{ mm}^3$. (A) normal saline administration (NSS-28), (B) zoledronate plus dexamethasone administration (Zol-28).

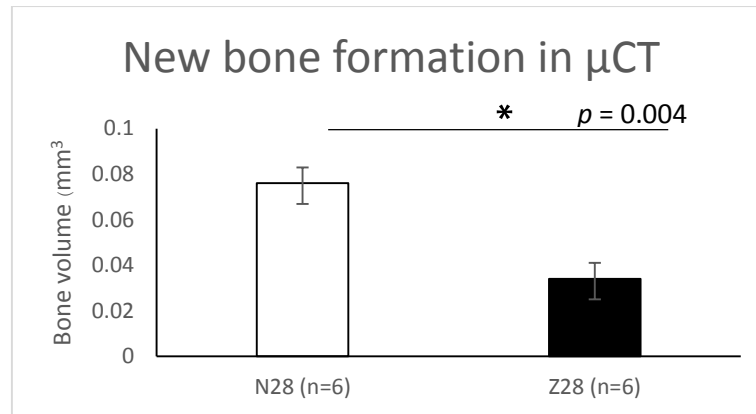


Figure 14 New bone formation (mm³) at Day 28 after extraction analyzed by μ CT in each group (data calculated per socket; n=12).

Histological analysis

Histological images showed complete epithelial coverage and normal wound healing in the control group (Figure 15A). Whereas, a lack of epithelial lining and poor bone formation were observed in the extraction socket of BP-treated group (Figure 15B). There was also detectable bacterial colonization and found abundant inflammatory cells in extraction sites of the BP-treated animals four weeks after extraction (Figure 15B). Histopathological images also demonstrated the higher number of empty osteocyte lacunae in BP-treated group compared to the control group (Figure 15 C, D). Percentage of normal osteocyte in Zol-0, NSS-0, NSS-14 and NSS-28 was not significantly different (90.6%, 88.89%, 70.8% and 85.49%, respectively), while The highest percentage of empty osteocyte in lacunae was observed in Zol-28 group followed by Zol-14 (47.5% and 24.8%, respectively) (Figure 16). The percentage of empty osteocyte lacunae was significantly higher in Zol-28 than NSS-28 group (47.5% (SE 5.1%) and 12.75% (SE 6.2%)), (P 0.005) (Figure 17).

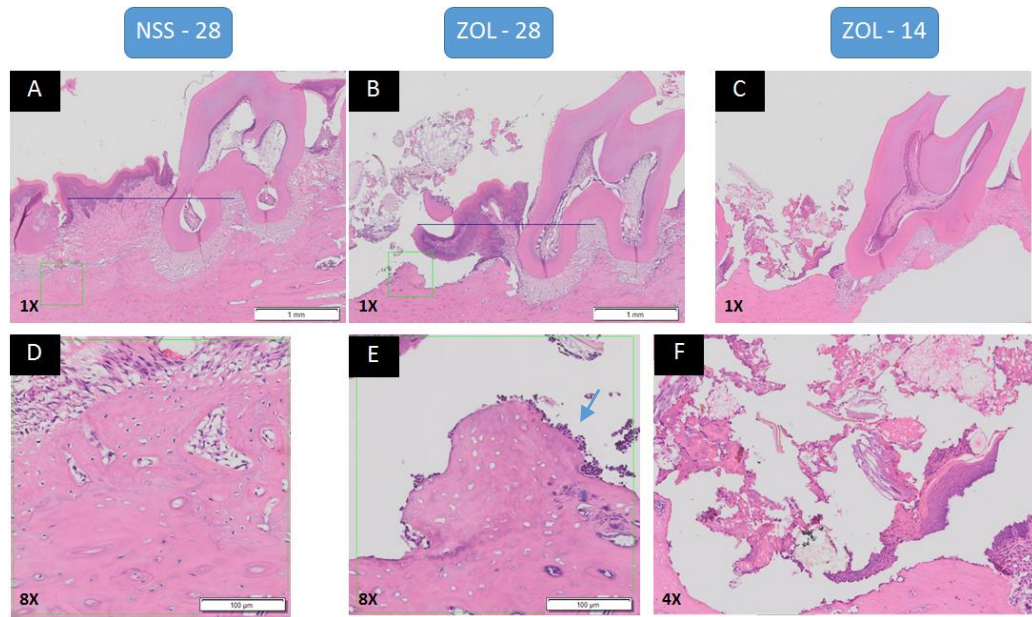


Figure 15 Histological images demonstrated complete epithelial lining and bone healing was found in the control group after 28-day extraction (A). A lack of mucosal coverage in the extraction socket, abundant of infiltrated cell (arrow), and abnormal bone remodeling could be observed in Zol group after 28 days of extraction. (B); scale bar: 100 μ m. Enlarged images of the square areas in 10X (D-F); scale bar: 1 mm.

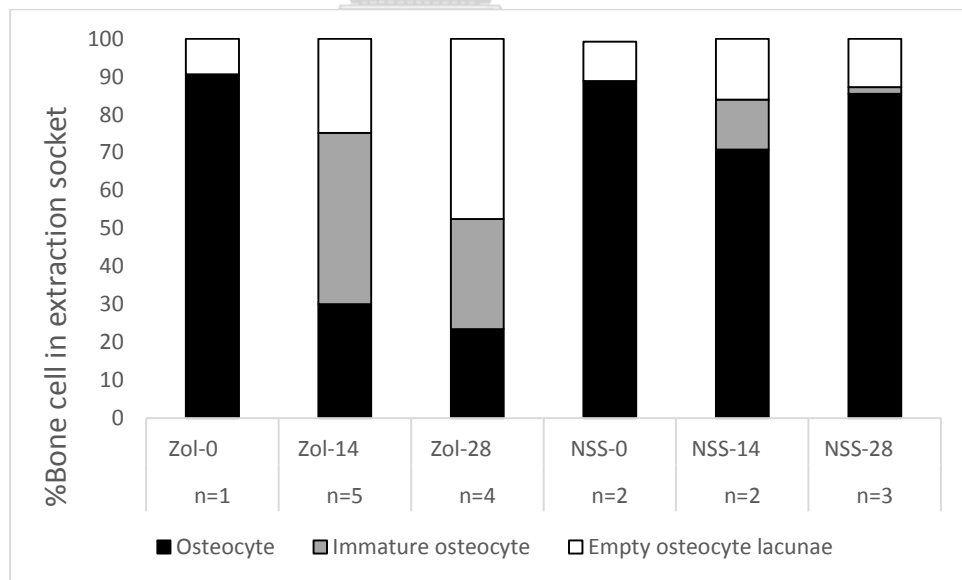


Figure 16 Percentage of bone formation cells determined at Baseline, Day 14 and Day 28 after extraction (N=17).

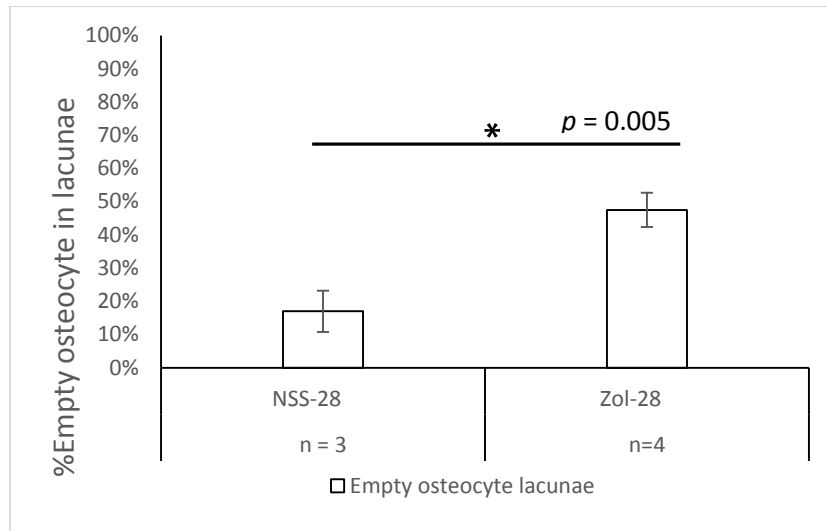


Figure 17 Percentage of osteocyte in lacunae determined at Day 28 after extraction (N=6).

miRNA analysis

For miRNA analysis, the miRNA expression level in bone tissue samples obtained from Zol-treated group and NSS-group at Day 28 after tooth extraction were compared. From total 8 candidate miRNAs, 5 miRNAs showed the upregulated expression in customized miRNA PCRarray. miR-23b-3p, miR-27-3p and miR-23a-3p that involved in an inhibition of osteoblastic activity were 4 to 2 folds upregulated in zoledronate plus dexamethasone treated group. In addition, miR-34a-5p that involved in osteoblastic differentiation, osteoclastogenesis and angiogenic process were 3.42-fold upregulation. A Low expression was found in miR-24a-3p (1.26-fold upregulation). In contrast, the downregulations were observed in miR-663a, miR652-3p and miR720 (1.71, 1.84 and 3.2-fold, respectively) (Figure 18 and 19).

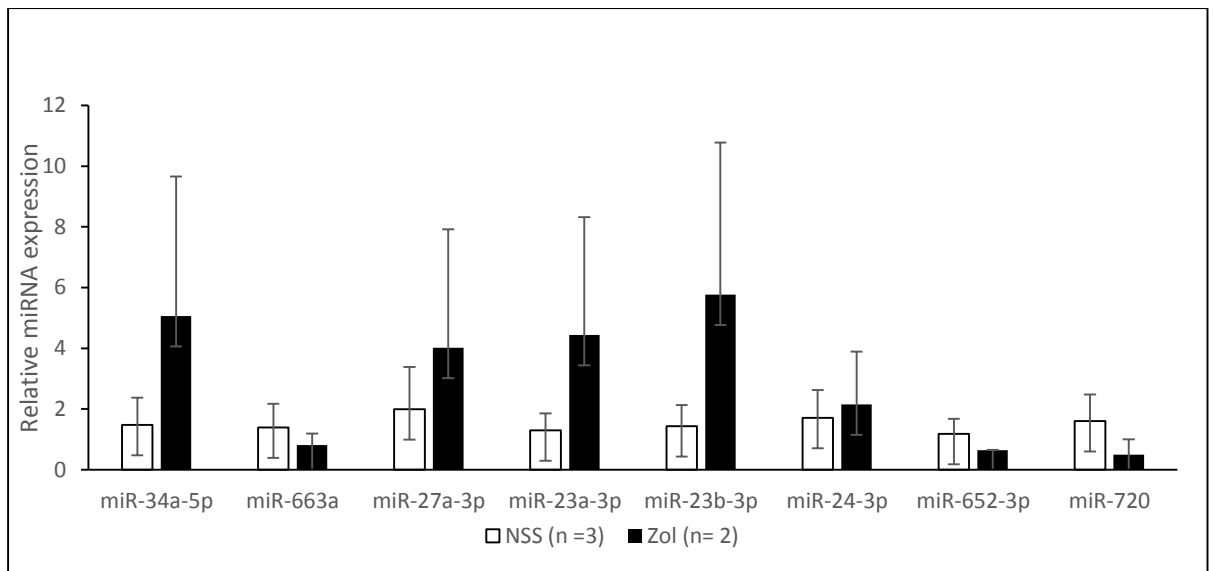


Figure 18 The relative expressions of candidate miRNAs in Zol-treated group and control group (NSS-group) at Day 28 post-extraction (N=5).

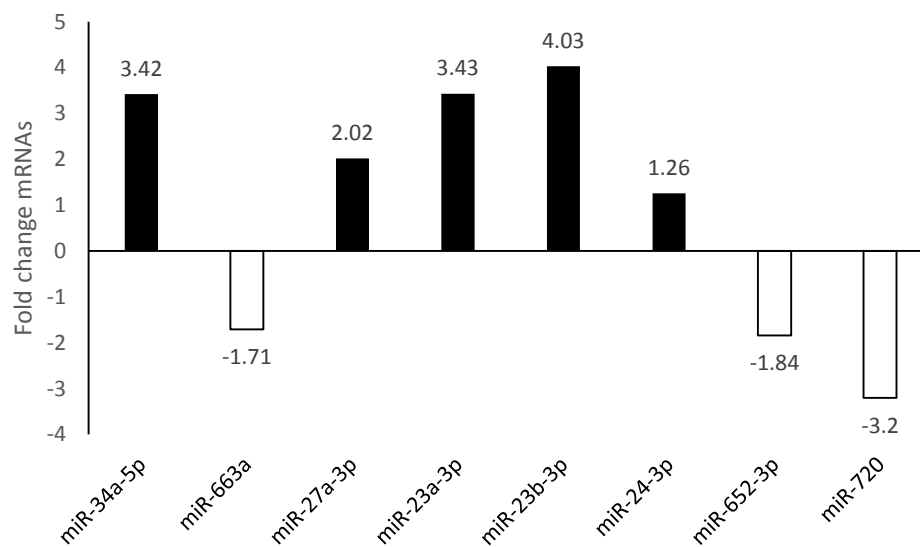


Figure 19 The fold change miRNAs comparison between Zol-treated group and control group (NSS-group) at Day 28 post-extraction (N=5).

Chapter V

Discussion

Bisphosphonate-related osteonecrosis of the jaw (MRONJ) has been discovered for many years. However, the mechanism of action of MRONJ either cellular and molecular knowledge is still unclear. Nevertheless, many studies have attempted to manage this disease with several regimens for MRONJ patients, those are only alleviated care. In this study, the MRONJ was established by an administration of zoledronate plus dexamethasone in SD rat models. The expressions of miRNAs targeted at angiogenic, osteoblastic, and osteoclastic activity in MRONJ-bone tissue samples were investigated.

According to the definition of MRONJ in human is exposed bone, having fistula, incomplete wound healing and epithelial lining for more than 8 weeks (Ruggiero et al., 2014). In this present study, the established MRONJ lesion in rat models could be observed by gross visualization showing an incomplete mucosal coverage and necrotic bone at 2 and 4 weeks after extraction. This similar timepoint of MRONJ occurrence has been reported in previous studies of rat models treated with zoledronate injection (Howie et al., 2015; Kaibuchi et al., 2016; Kuroshima et al., 2018).

In this study, the effect of using zoledronate plus dexamethasone for cancer treatment influenced on reduced weight gain rate at all time-points compared to the control. Consistent with the claim by FDA that the side effect of zoledronic injection using occurred to 16% weight loss and 13% appetite decrease after drug prescription (Corporation, 2005).

A micro-CT analysis of hard tissue characteristics revealed the poorly formed bony structure in the extraction socket of rats receiving zoledronate-dexamethasone injection as shown in the 3D rendering images compared to the control groups. To quantify the healing capacity of alveolar bone, the bone volume in extraction sockets at day 28 post-extraction were calculated. The bone volume of Zol-group observed at day 28 were smaller than NSS-group observed at day 28. In this study, two-fold smaller bone volume could be observed in Zol-28 group compared to NSS-28 group. Kuroshima et al., 2018 also reported the 50% lesser bone fill in extraction sockets after being injected with zoledronate/cyclophosphamide than those of a control group at 7

weeks after extraction (Kuroshima et al., 2018). Another similar study also demonstrated a percentage of calcification volume in extraction sockets of zoledronate/dexamethasone-treat group was twice lower than the untreated group (Kaibuchi et al., 2016). The differences in results may be due to different types of the rat used, drug administration, and calculation methods. Interestingly, within Zol-groups, a bone volume of healing sockets after tooth extraction for 28 days was twice smaller than 14-day extraction sockets. This result ensured the method in establishing MRONJ lesion and also suggested that the MRONJ occurrence could be early notified at 2 weeks after tooth extraction in rat models.

In histological study, H&E staining demonstrated normal wound healing with intact epithelium and connective tissue in the extraction socket of NSS-group while in 28-day zoledronate treated groups showed incomplete wound healing, detached epithelium and dense inflammatory cells infiltration. The healing of alveolar sockets in NSS group demonstrated new bone formation with 85.5% healthy osteocytes in lacunae. In contrast, a number of empty osteocyte lacunae was remarkably higher in Zol-28 group which showed 55.6% empty lacunae. This result corresponded with previous study that approximately 3-fold higher number of empty osteocyte lacunae could be observed comparing with that of the control NSS group (Kuroshima et al., 2018).

To understand a molecular mechanism controlling the pathogenesis of MRONJ, the roles of miRNAs in MRONJ development have been studied. As the key mechanisms that propagate MRONJ are an inhibition of angiogenesis and a promotion of osteoclastic activity, 8 candidate miRNAs that previously reported as having roles in angiogenic activity and bone remodeling were chosen and evaluated. In this study, miRNAs targeting at RUNX2 (Runt-related transcription factor 2) suppression including miR-23a-3p, miR-23b-3p, miR27a-3p and miR-24-3p were found to be upregulated. Previous studies have demonstrated the miR-23a~27a~24-2 cluster was one of 11 miRNAs that has been identified as negative tuning on RUNX2 which in turn suppressing osteoblast differentiation (Zhang et al., 2011) (Lian et al., 2012). An inhibitory role of the miR-23a on RUNX2 and special AT-rich sequence-binding protein-2 (SATB2) in mesenchymal cells has been reported, which resulting in suppression of osteoblast

maturation (Zhang et al., 2011). In MRONJ rat models, miR23a has been noted as one of the candidate circulating biomarkers to diagnose MRONJ (Yang et al., 2018). Likewise, miR-27a has been reported as having a role in inhibiting Hoxa10 gene that control RUNX2 resulted in decreasing osteoblastogenesis (Lian et al., 2012). The result from this study indicated the role of miR-23a-3p, miR-23b-3p, miR27a-3p and miR-24-3p in impeding an osteoblastic maturation in MRONJ.

Other miRNAs that affect MRONJ mechanism by impairing angiogenesis process were miR-663, miR-652 and miR-720. Previous studies hypothesized that miR-720 and miR-663 could promote angiogenesis. Wang et al., 2014 induced the expression of miR-720 and vasohibin1 (VASH1) by infrared therapy resulted in stimulating of endothelial cell migration and vascular formation (Wang et al., 2014). In addition, miR-663 promoted endothelial cell proliferation via ATF4 (Afonyushkin et al., 2012). In contrast, Hong et al. reported an anti-angiogenic effect of miR-663. The up-regulation of miR-663 was found in atherosclerotic plaque and the knockout of miR-663 resulted in promoting a repair of vascular endothelium via transforming growth factor beta 1 (TGF- β 1) in hyperuricemic rat model (Hong et al., 2015). The down-regulated expression of pro-angiogenic miRNA in zoledronate-treated group observed in this study might relate to the interruption of blood vessel formation that usually occurred in MRONJ process. In terms of miR-652-3p, our study observed the 1.8-fold down-regulated expression comparing with a control group. This result contradicted to one previous study by Huang et al. that reported an inhibitory role of miR-652-3p in endothelial cell migration and proliferation observed in an atherosclerotic plaque in a knockout mice study (Huang et al., 2019). In bone tissue, a role of miR-652-3p in angiogenesis has never been reported. However, due to a limited sample size in this present study. Further experiment is needed to elucidate an effect of miR-652-3p.

According to the researches, our study suggested the role of miR-34 involving in both bone remodeling and anti-angiogenic activity that occurred in MRONJ. The 3.42-fold up-regulation of miR-34a-5p expression was observed in MRONJ extraction sockets. In irradiated bone defect, miR-34a could promote bone regeneration by inducing an osteoblastic differentiation of bone marrow stromal cells (BSMCs) via NOTCH1 targeting (Liu et al., 2019) and blocking osteoclastogenesis via inhibited Tgif2 (Krzyszinski et al.,

2014). In angiogenesis, miR-34a-5p decreased the number of vessels by inhibiting a function of silence information regulator 1 (SIRT1) (Ito et al., 2010).

Pathogenesis of MRONJ in blood vessel regeneration, bone formation and resorption was performed in this research. However, several limitations should be considered in this study. Due to the COVID-19 pandemic situation, some parts of the experimental plan were disturbed and could not be performed. The number of study samples is limited because of the death of animals during study and lack of the third-time repetitive study. Therefore, a statistical significance analysis could not be applied to strengthen the results. Furthermore, an immunohistochemical study should be performed in order to evaluate the function of osteoclast and also the number of blood vessels. In terms of miRNA analysis, there are still several miRNAs that might associate with the pathophysiological mechanism of MRONJ to be investigated; for example, miRNAs involved in promoting osteoclastic activity such as miR-21 and miR-31 or other miRNAs that have an influence on angiogenic activity, including miR-221, miR-126, miR-210 and miR-278. Altogether, future further investigation with a larger sample size will confirm the results from this study and provide an insightful information regarding the miRNA profile in bone tissue of MRONJ. An application of miRNA may warrant a future therapeutic approach for MRONJ patients.



Chapter VI

Conclusion

In this study, the MRONJ was successfully developed in the SD rat model when treated with BPs. Candidate miRNAs were found to be involving in the development of MRONJ. miRNAs that affected an inhibition of osteoblast maturation, including miR-23a-3p, miR-23b-3p, miR27a-3p and miR-24-3p were upregulated in MRONJ bone tissue samples. Proangiogenesis-relating miRNAs such as miR-663a and miR-720 were down regulation in the MRONJ extraction sockets. The expression of miR-34 that had dual effects on both bone remodeling and blood vessel formation was upregulated. This study suggested that the certain miRNAs have a role in controlling the cellular functions related to bone remodeling mechanisms and angiogenic activity in MRONJ. Still, a variety of miRNAs, particularly osteoclastogenesis-related miRNAs, are of needed to be clarified their functions in which associated with pathophysiologic mechanisms of MRONJ.

Appendix

Information of animal model

Species : Rattus Norvegicus

Strain/Stock : Sprague Dawley

Age and Weight : 8 weeks , 200 – 250 g

Quarantine period : 2 weeks

Body weight (g) : lot 2 only

RAT	baseline	Week1	Week2 (extraction)	Week3	Week4	Week6
001	155	189	177	180	185	215
002	155	174	177.42	165	172	197.5
003	155	175	177.18	155	175	-
004	155	181	183.87	184	182	-
005	155	174	198	-	-	-
006	155	193	197	195	185.5	-
007	155	219	232	239	250.5	-
008	155	215	228	-	-	-
009	155	221	240	251	259	286
010	155	220	232	241	248.5	275
total	155	196.1	204.25	201.25	207.19	243.38
Z	155	178.6	182.69	171	178.5	206.25
N	155	213.6	225.8	231.5	235.88	280.5

Protocol Drug injection

Intervention

Drug	Route of administration	Dose	Remark
Zometa	Intraperitoneal	0.33 ml	26-27G
Dexton		0.25 ml	
Normal saline		0.05 ml	
Dexton	Intraperitoneal	0.25 ml	26-27G
Normal saline		0.40 ml	
Normal saline	Intraperitoneal	0.65 ml	26-27G

Note: Injected once every Monday, Wednesday, and Friday for 4 weeks

General anesthesia before operation

Drug	Route of administration	Dose	Remark
Zoletil	Intraperitoneal	40 mg/kg in 100 ml injected 0.1 ml	26-27G
Xylazine	Intraperitoneal	2 mg/kg in 5 ml injected 0.1 ml	26-27G
Carpofen	Subcutaneous	4 mg/kg, used 5 mg/ml injected 0.2 ml	26-27G
Enrofloxacin	Subcutaneous	10 mg/kg used 5 mg/ml injected 0.5 ml	26-27G

Analgesia

Drug	Route of administration	Dose	Remark
Tramadol	Subcutaneous	4 mg/kg 0.02 ml b.i.d.	26-27G

Note: Injected Tramadol 2 times/day for 3 days

Protocol for blood withdrawal

Technic	Route of administration	Dose	Remark
Blood collection	Lateral tail vein	0.3 ml	22-23G May need butterfly needle
Blood collection	Cardiac	5 ml	21G

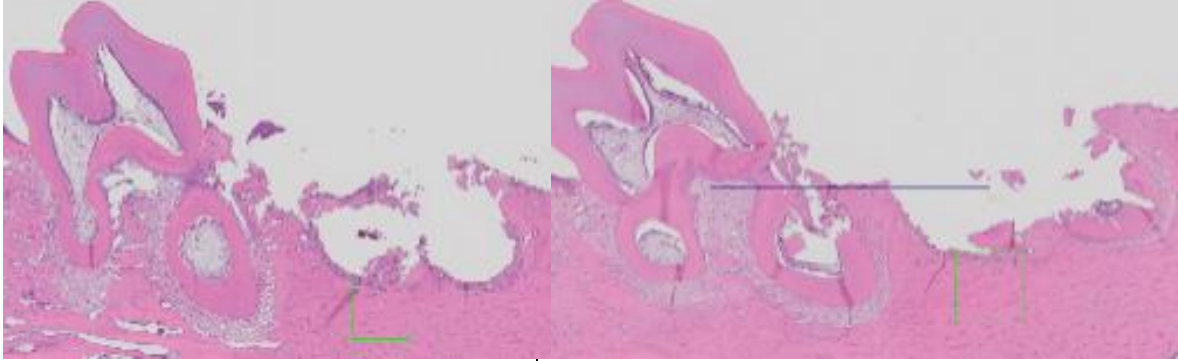
Cardiac puncture

1. CO₂ inhalation
2. Check all reflex, clean skin surface with alcohol
3. Cut through midline skin and muscle with scissors at xiphoid process
4. Collect 2-3 mL cardiac blood with 21, 23G needle, bevel down (right atrium is preferable)
5. Keep blood sample in EDTA tube

Table2 Designed primer of candidate miRNAs

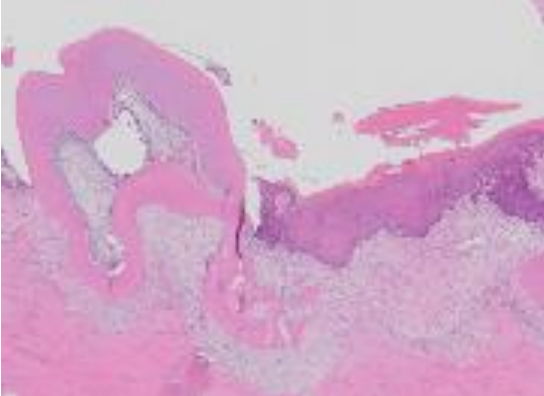
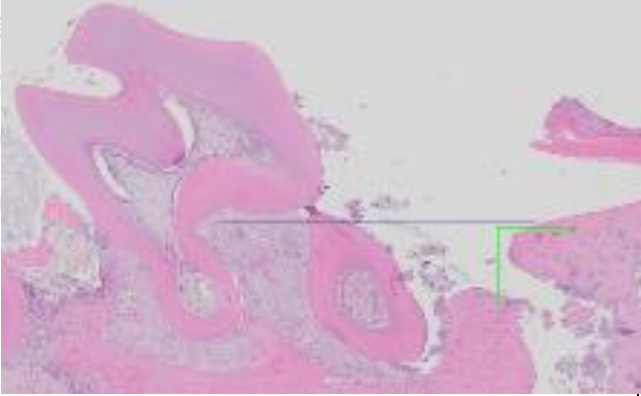
miRBase Accession No.	Mature miRNA ID	miScript Primer Assay Catalog
MIMAT0000255	hsa-miR-34a-5p	MS00003318
MIMAT0003322	hsa-miR-652-3p	MS00010451
MIMAT0003326	hsa-miR-663a	MS00037247
MIMAT0005954	hsa-miR-720	MS00014833
MIMAT0000078	hsa-miR-23a-3p	MS00031633
MIMAT0000418	hsa-miR-23b-3p	MS00031647
MIMAT0000084	hsa-miR-27a-3p	MS00003241
MIMAT0000080	hsa-miR-24-3p	MS00006552

Gross, micro-CT and histological data
Day 0 after extraction as baseline

Gross	NSS	Zometa+Dex
		
Microct		
Histology		

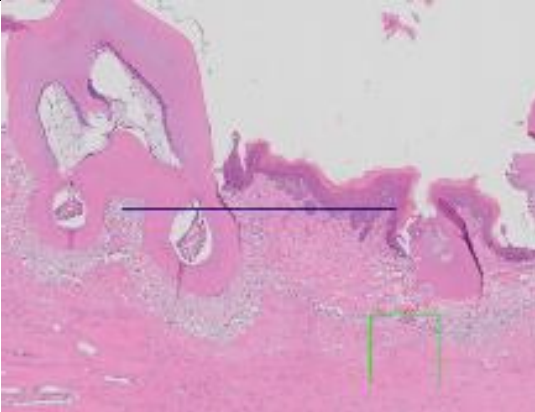
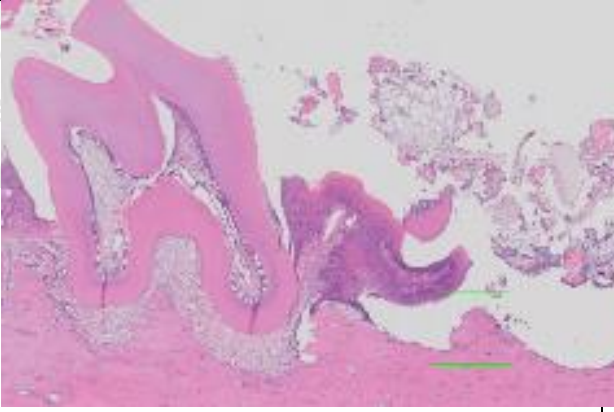
Note: retained roots from μ CT were excluded from μ CT analysis and sample in μ CT were calculated per socket (not per rat)

Day 14 after extraction

Gross	NSS	Zometa+Dex
Microct		
Histology		

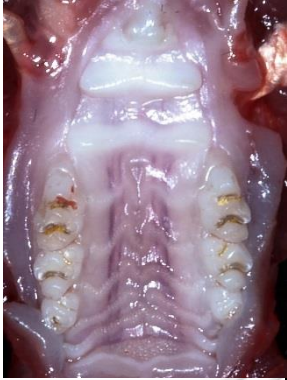
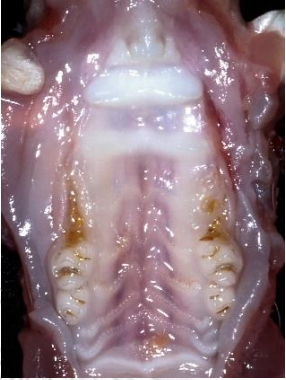
Note: retained roots from μ CT were excluded from μ CT analysis and sample in μ CT were calculated per socket (not per rat)

Day 28 after extraction

Gross	Nss	Zometa+Dex
Microct		
Histology		

Note: retained roots from μ CT were excluded from μ CT analysis and sample in μ CT were calculated per socket (not per rat)

Table 3. Comparison of gross specimen in each timeline

NSS	Day 0	Day 14	Day 28
			
Zol + Dex			

Results in PCRArray

Average CT	909Z	002Z	916N28	9	010N	914	008N0	006N
	Z28	Z28	N28	N28	N28	N0	N0	N14
miR-34a-5p	28.78	35.82	37.3	37.58	0.00	37.57	37.79	37.81
miR-663a	30.3	34.47	0	35.05	36.84	35.03	35.66	37.21
miR-27a-3p	25.85	34.63	33.51	33.09	36.07	32.58	37.52	35.26
miR-23a-3p	22.52	29.08	32.21	28.52	32.17	28.67	29.90	31.21
miR-23b-3p	24.13	30.61	34.11	30.27	34.47	30.95	31.10	32.81
miR-24-3p	24.54	30.46	32.83	28.88	33.97	30.27	30.00	32.40
miR-652-3p	30.06	32.71	36.83	32.41	35.14	36.55	34.45	0.00
miR-720	30.11	24.65	28.48	24.40	29.16	26.52	27.26	28.20
U6	20.96	26.03	31.55	27.47	28.41	30.58	28.28	28.31



miRNA concentration from Nanodrop (Bone)

Rat No. lot1	Yield ng/ μ l	260/280	260/230	Drug/Day after extraction
905	254.9	2.02	1.75	Z/D14
906	198.1	1.93	1.28	Z/D14
907	655.5	2.00	1.63	Z/D14
908	-	-	-	Z/D28
909	147.1	2.07	0.73	Z/D28
910	152.9	1.92	0.38	Z/D28
914	49.3	2.34	0.70	N/D0
916	69.6	2.29	0.63	N/D28
917	71.7	1.85	0.49	N/D2

Note :

908 : Death during blood sample collection

917 : Death during experiment

Total 17 rats included in this study (Lot 1 + 2)

Rat No. lot2	Yield ng/ μ l	260/280	260/230	Drug/Day after extraction
001	463.7	2.04	1.84	Z/D28
002	234.8	2.08	1.69	Z/D28
003	352.4	2.08	1.92	Z/D14
004	464.7	2.07	1.84	Z/D14
005	58.4	1.99	0.69	Z/D0
006	435.8	2.05	1.29	N/D14
007	358.2	2.05	1.70	N/D14
008	163.9	2.01	1.09	N/D0
009	634.6	2.04	1.39	N/D28
010	344.2	2.08	1.39	N/D28

% Osteocyte in lacunae in ROI observed by H&E staining

N=15	Osteocyte	Premature osteocyte	Empty osteocyte in lacunae
Z0 n=1	90.6	0	9.4
Z14 n=4	15.81	51.75	32.45
Z28 n=3	5.33	39.11	55.56
N0 n=2	88.89	0	10.34
N14 n=2	70.8	13.14	16.06
N28 n=3	85.49	1.77	12.75

	Osteocyte number	Oseocyte percent	Immature Osteocyte number	Immature Osteocyte percent	Empty osteocyte number	Empty osteocyte percent	Total number	Total percent
001Z	5	4	41	34	75	62	121	100
002Z	8	9	29	32.58	52	58.42	89	100
003Z	4	3.78	57	53.77	45	42.45	106	100
004Z	98	80.33	4	3.28	20	16.39	122	100
005Z	106	90.6	0	0	11	9.4	117	100
006N	96	70.07	18	13.14	23	17.79	137	100
007N	98	71.53	18	13.14	21	15.33	137	100
008N	89	88.12	0	0	12	11.88	101	100
009N	109	78.42	1	0.72	29	20.86	139	100
010N	99	79.2	5	4	21	16.8	125	100
905Z	27	37.5	27	37.5	18	25	72	100
906Z	2	3.85	26	50	24	46.15	52	100
907Z	19	18.1	69	65.71	17	16.19	105	100
909Z	2	2.98	34	50.75	31	46.27	67	100
910Z	79	66.39	8	6.72	32	26.89	119	100
914N	78	89.66	0	0	9	10.34	87	100
916N	171	98.84	1	0.58	1	0.58	173	100

Result micro – CT (bone volume)

Lot1			Lot2				
Z28	Z14	N28	Z28	Z14	N28	N14	
0.0186	0.0098	0.1016	0.0447	0.0989	0.0776	0.0484	
0.0068	0.0497	0.0869	0.0311		0.0572	0.0931	
0.0332	0.0758		0.0709		0.0776	0.0484	
					0.0572	0.0868	
Average	0.019533	0.0451	0.09425	0.0489	0.0989	0.0674	0.069175

Total	Z28 (n=6)	Z14 (n=4)	N28 (n=6)	N14 (n=4)
Average	0.034217	0.05855	0.07635	0.07512
SE	0.0091	0.0191	0.07	0.011

Statistics

Histo analysis

Independent Samples Test										
		Levene's Test for Equality of Variances		t-test for Equality of Means						
		F	Sig.	t	df	Sig. (2-tailed)	Mean Difference	Std. Error Difference	95% Confidence Interval of the Difference	
									Lower	Upper
OIL	Equal variances assumed	.410	.557	5.480	4	.005	42.81667	7.81282	21.12481	64.50853
	Equal variances not assumed			5.480	3.751	.006	42.81667	7.81282	20.54538	65.08795



Micro – CT analysis

Independent Samples Test										
		Equality of Variances		t-test for Equality of Means						
		F	Sig.	t	df	Sig. (2-tailed)	Mean Difference	Std. Error Difference	of the Difference	
									Lower	Upper
bone volume	Equal variances assumed	.176	.683	-3.673	10	.004	-.04213333	.01147069	-.06769163	-.01657504
	Equal variances not assumed			-3.673	9.423	.005	-.04213333	.01147069	-.06790521	-.01636146

miRNA analysis

		Equality of Variances		t-test for Equality of Means						
		F	Sig.	t	df	Sig. (2-tailed)	Mean Difference	Std. Error Difference	Interval of the	
									Lower	Upper
mir34	Equal variances assumed	68.111	.004	-.992	3	.395	-3.58000	3.61048	-15.07015	7.91015
	Equal variances not assumed			-.766	1.076	.577	-3.58000	4.67619	-53.89359	46.73359
mir663a	Equal variances assumed	3.349	.165	.545	3	.624	.57333	1.05210	-2.77491	3.92157
	Equal variances not assumed			.657	2.746	.562	.57333	.87202	-2.35298	3.49964
mir27a3p	Equal variances assumed	9.076	.057	-.588	3	.598	-2.02500	3.44341	-12.98347	8.93347
	Equal variances not assumed			-.488	1.278	.696	-2.02500	4.15069	-34.08491	30.03491
mir23a3p	Equal variances assumed	97.349	.002	-1.018	3	.384	-3.04167	2.98759	-12.54951	6.46618
	Equal variances not assumed			-.776	1.047	.575	-3.04167	3.91993	-47.87314	41.78980

mir23b3p	Equal variances assumed	118.133	.002	-1.180	3	.323	-4.46833	3.78541	-16.51519	7.57852
	Equal variances not assumed			-.891	1.025	.534	-4.46833	5.01641	-64.60016	55.66350
mir243p	Equal variances assumed	.960	.399	-.252	3	.817	-.44500	1.76508	-6.06228	5.17228
	Equal variances not assumed			-.226	1.592	.847	-.44500	1.96879	-11.37620	10.48620
mir6523p	Equal variances assumed	9.100	.057	.827	3	.469	.54000	.65286	-1.53768	2.61768
	Equal variances not assumed			1.068	2.002	.397	.54000	.50577	-1.63451	2.71451
mir720	Equal variances assumed	1.165	.360	.927	3	.422	1.10667	1.19360	-2.69191	4.90524
	Equal variances not assumed			1.095	2.898	.356	1.10667	1.01068	-2.17500	4.38833

REFERENCES



จุฬาลงกรณ์มหาวิทยาลัย
CHULALONGKORN UNIVERSITY

- Afonyushkin, T., O.V. Oskolkova, and V.N. Bochkov. 2012. Permissive role of miR-663 in induction of VEGF and activation of the ATF4 branch of unfolded protein response in endothelial cells by oxidized phospholipids. *Atherosclerosis*. 225:50-55.
- Altuvia, Y., P. Landgraf, G. Lithwick, N. Elefant, S. Pfeffer, A. Aravin, M.J. Brownstein, T. Tuschl, and H. Margalit. 2005. Clustering and conservation patterns of human microRNAs. *Nucleic acids research*. 33:2697-2706.
- Bartel, D.P. 2004. MicroRNAs: genomics, biogenesis, mechanism, and function. *cell*. 116:281-297.
- Black, D.M., P.D. Delmas, R. Eastell, I.R. Reid, S. Boonen, J.A. Cauley, F. Cosman, P. Lakatos, P.C. Leung, and Z. Man. 2007. Once-yearly zoledronic acid for treatment of postmenopausal osteoporosis. *New England Journal of Medicine*. 356:1809-1822.
- Black, D.M., A.V. Schwartz, K.E. Ensrud, J.A. Cauley, S. Levis, S.A. Quandt, S. Satterfield, R.B. Wallace, D.C. Bauer, and L. Palermo. 2006. Effects of continuing or stopping alendronate after 5 years of treatment: the Fracture Intervention Trial Long-term Extension (FLEX): a randomized trial. *Jama*. 296:2927-2938.
- Center, J.R., D. Bliuc, N.D. Nguyen, T.V. Nguyen, and J.A. Eisman. 2011. Osteoporosis medication and reduced mortality risk in elderly women and men. *The Journal of Clinical Endocrinology & Metabolism*. 96:1006-1014.
- Coleman, R.E., H. Marshall, D. Cameron, D. Dodwell, R. Burkinshaw, M. Keane, M. Gil, S.J. Houston, R.J. Grieve, and P.J. Barrett-Lee. 2011. Breast-cancer adjuvant therapy with zoledronic acid. *New England Journal of Medicine*. 365:1396-1405.
- Corporation, N.P. 2005. Zometa®(Zoledronic Acid)[prescribing information].
- Das, S.G., M. Romagnoli, N.D. Mineva, S. Barillé-Nion, P. Jézéquel, M. Campone, and G.E. Sonenshein. 2016. miR-720 is a downstream target of an ADAM8-induced ERK signaling cascade that promotes the migratory and invasive phenotype of triple-negative breast cancer cells. *Breast Cancer Research*. 18:40.
- Delmas, P., C. Benhamou, Z. Man, W. Tlustochowicz, E. Matzkin, R. Eusebio, J. Zanchetta, W. Olszynski, R. Recker, and M. McClung. 2008a. Monthly dosing of

- 75 mg risedronate on 2 consecutive days a month: efficacy and safety results. *Osteoporosis International*. 19:1039-1045.
- Delmas, P.D., M.R. McClung, J.R. Zanchetta, A. Racewicz, C. Roux, C.-L. Benhamou, Z. Man, R.A. Eusebio, J.F. Beary, and D.E. Burgio. 2008b. Efficacy and safety of risedronate 150 mg once a month in the treatment of postmenopausal osteoporosis. *Bone*. 42:36-42.
- Drake, M.T., B.L. Clarke, and S. Khosla. 2008. Bisphosphonates: mechanism of action and role in clinical practice. *In Mayo Clinic Proceedings*. Vol. 83. Elsevier. 1032-1045.
- Drieling, R.L., A.Z. LaCroix, S.A. Beresford, D.M. Boudreau, C. Kooperberg, R.T. Chlebowski, M. Gass, C.J. Crandall, C.R. Womack, and S.R. Heckbert. 2016. Long-term oral bisphosphonate use in relation to fracture risk in postmenopausal women with breast cancer: findings from the Women's Health Initiative. *Menopause*. 23:1168-1175.
- E Dunford, J. 2010. Molecular targets of the nitrogen containing bisphosphonates: the molecular pharmacology of prenyl synthase inhibition. *Current pharmaceutical design*. 16:2961-2969.
- Fan, C., L. Jia, Y. Zheng, C. Jin, Y. Liu, H. Liu, and Y. Zhou. 2016. MiR-34a promotes osteogenic differentiation of human adipose-derived stem cells via the RBP2/NOTCH1/CYCLIN D1 coregulatory network. *Stem cell reports*. 7:236-248.
- Fasanaro, P., Y. D'Alessandra, V. Di Stefano, R. Melchionna, S. Romani, G. Pompilio, M.C. Capogrossi, and F. Martelli. 2008. MicroRNA-210 modulates endothelial cell response to hypoxia and inhibits the receptor tyrosine kinase ligand Ephrin-A3. *Journal of Biological Chemistry*. 283:15878-15883.
- Filleul, O., E. Crompton, and S. Saussez. 2010. Bisphosphonate-induced osteonecrosis of the jaw: a review of 2,400 patient cases. *Journal of cancer research and clinical oncology*. 136:1117-1124.
- Fish, J.E., M.M. Santoro, S.U. Morton, S. Yu, R.-F. Yeh, J.D. Wythe, K.N. Ivey, B.G. Bruneau, D.Y. Stainier, and D. Srivastava. 2008. miR-126 regulates angiogenic signaling and vascular integrity. *Developmental cell*. 15:272-284.

- Förstermann, U., and T. Münzel. 2006. Endothelial nitric oxide synthase in vascular disease: from marvel to menace. *Circulation*. 113:1708-1714.
- Ganda, K. 2013. *Dentist's Guide to Medical Conditions, Medications and Complications*. John Wiley & Sons.
- Graziani, F., P. Vescovi, G. Campisi, G. Favia, M. Gabriele, G.M. Gaeta, S. Gennai, F. Goia, M. Miccoli, and F. Peluso. 2012. Resective surgical approach shows a high performance in the management of advanced cases of bisphosphonate-related osteonecrosis of the jaws: a retrospective survey of 347 cases. *Journal of Oral and Maxillofacial Surgery*. 70:2501-2507.
- Harris, T.A., M. Yamakuchi, M. Ferlito, J.T. Mendell, and C.J. Lowenstein. 2008. MicroRNA-126 regulates endothelial expression of vascular cell adhesion molecule 1. *Proceedings of the National Academy of Sciences*. 105:1516-1521.
- Hassan, M.Q., J.A. Gordon, M.M. Beloti, C.M. Croce, A.J. Van Wijnen, J.L. Stein, G.S. Stein, and J.B. Lian. 2010. A network connecting Runx2, SATB2, and the miR-23a~27a~24-2 cluster regulates the osteoblast differentiation program. *Proceedings of the National Academy of Sciences*. 107:19879-19884.
- He, L., J.M. Thomson, M.T. Hemann, E. Hernando-Monge, D. Mu, S. Goodson, S. Powers, C. Cordon-Cardo, S.W. Lowe, and G.J. Hannon. 2005. A microRNA polycistron as a potential human oncogene. *nature*. 435:828.
- Hong, Q., S. Yu, X. Geng, L. Duan, W. Zheng, M. Fan, X. Chen, and D. Wu. 2015. High Concentrations of Uric Acid Inhibit Endothelial Cell Migration via miR-663 Which Regulates Phosphatase and Tensin Homolog by Targeting Transforming Growth Factor- β 1. *Microcirculation*. 22:306-314.
- Howie, R.N., J.L. Borke, Z. Kurago, A. Daoudi, J. Cray, I.E. Zakhary, T.L. Brown, J.N. Raley, L.T. Tran, and R. Messer. 2015. A model for osteonecrosis of the jaw with zoledronate treatment following repeated major trauma. *PloS one*. 10.
- Hua, Z., Q. Lv, W. Ye, C.-K.A. Wong, G. Cai, D. Gu, Y. Ji, C. Zhao, J. Wang, and B.B. Yang. 2006. MiRNA-directed regulation of VEGF and other angiogenic factors under hypoxia. *PloS one*. 1:e116.

- Huang, R., Z. Hu, Y. Cao, H. Li, H. Zhang, W. Su, Y. Xu, L. Liang, N. Melgiri, and L. Jiang. 2019. MiR-652-3p inhibition enhances endothelial repair and reduces atherosclerosis by promoting Cyclin D2 expression. *EBioMedicine*. 40:685-694.
- Irwandi, R.A. 2015. MICRORNA-302A-3P REGULATES PROSTAGLANDIN E2-INDUCED RANK LIGAND EXPRESSION IN HUMAN MANDIBULAR BONE-DERIVED CELLS. Chulalongkorn University.
- Ito, T., S. Yagi, and M. Yamakuchi. 2010. MicroRNA-34a regulation of endothelial senescence. *Biochemical and biophysical research communications*. 398:735-740.
- Jeyaseelan, K., K.Y. Lim, and A. Armugam. 2008. MicroRNA expression in the blood and brain of rats subjected to transient focal ischemia by middle cerebral artery occlusion. *Stroke*. 39:959-966.
- Kagiya, T., and S. Nakamura. 2013. Expression profiling of microRNAs in RAW264. 7 cells treated with a combination of tumor necrosis factor alpha and RANKL during osteoclast differentiation. *Journal of periodontal research*. 48:373-385.
- Kaibuchi, N., T. Iwata, M. Yamato, T. Okano, and T. Ando. 2016. Multipotent mesenchymal stromal cell sheet therapy for bisphosphonate-related osteonecrosis of the jaw in a rat model. *Acta biomaterialia*. 42:400-410.
- Khan, A.A., A. Morrison, D.A. Hanley, D. Felsenberg, L.K. McCauley, F. O'Ryan, I.R. Reid, S.L. Ruggiero, A. Taguchi, and S. Tetradis. 2015. Diagnosis and management of osteonecrosis of the jaw: a systematic review and international consensus. *Journal of Bone and Mineral Research*. 30:3-23.
- Krol, J., I. Loedige, and W. Filipowicz. 2010. The widespread regulation of microRNA biogenesis, function and decay. *Nat Rev Genet*. 11:597-610.
- Krzyszinski, J.Y., W. Wei, H. Huynh, Z. Jin, X. Wang, T.-C. Chang, X.-J. Xie, L. He, L.S. Mangala, and G. Lopez-Berestein. 2014. miR-34a blocks osteoporosis and bone metastasis by inhibiting osteoclastogenesis and Tgfb2. *Nature*. 512:431-435.
- Kühl, S., C. Walter, S. Acham, R. Pfeffer, and J.T. Lambrecht. 2012. Bisphosphonate-related osteonecrosis of the jaws—a review. *Oral oncology*. 48:938-947.

- Kuhnert, F., M.R. Mancuso, J. Hampton, K. Stankunas, T. Asano, C.-Z. Chen, and C.J. Kuo. 2008. Attribution of vascular phenotypes of the murine *Egfl7* locus to the microRNA miR-126. *Development*. 135:3989-3993.
- Kuijper, S., C.J. Turner, and R.H. Adams. 2007. Regulation of angiogenesis by Eph-ephrin interactions. *Trends in cardiovascular medicine*. 17:145-151.
- Kuroshima, S., M. Sasaki, K. Nakajima, S. Tamaki, H. Hayano, and T. Sawase. 2018. Transplantation of Noncultured Stromal Vascular Fraction Cells of Adipose Tissue Ameliorates Osteonecrosis of the Jaw-Like Lesions in Mice. *Journal of Bone and Mineral Research*. 33:154-166.
- Lee, D.Y., Z. Deng, C.H. Wang, and B.B. Yang. 2007. MicroRNA-378 promotes cell survival, tumor growth, and angiogenesis by targeting SuFu and Fus-1 expression. *Proc Natl Acad Sci U S A*. 104:20350-20355.
- Li, P., N. Zhu, B. Yi, N. Wang, M. Chen, X. You, X. Zhao, C.C. Solomides, Y. Qin, and J. Sun. 2013. MicroRNA-663 regulates human vascular smooth muscle cell phenotypic switch and vascular neointimal formation. *Circulation research*. 113:1117-1127.
- Li, Y., Y.-H. Song, F. Li, T. Yang, Y.W. Lu, and Y.-J. Geng. 2009. MicroRNA-221 regulates high glucose-induced endothelial dysfunction. *Biochemical and biophysical research communications*. 381:81-83.
- Lian, J.B., G.S. Stein, A.J. Van Wijnen, J.L. Stein, M.Q. Hassan, T. Gaur, and Y. Zhang. 2012. MicroRNA control of bone formation and homeostasis. *Nature Reviews Endocrinology*. 8:212.
- Liekens, S., E. De Clercq, and J. Neyts. 2001. Angiogenesis: regulators and clinical applications. *Biochemical pharmacology*. 61:253-270.
- Liu, H., Y. Dong, X. Feng, L. Li, Y. Jiao, S. Bai, Z. Feng, H. Yu, X. Li, and Y. Zhao. 2019. miR-34a promotes bone regeneration in irradiated bone defects by enhancing osteoblastic differentiation of mesenchymal stromal cells in rats. *Stem cell research & therapy*. 10:180.
- McClung, M., S.T. Harris, P.D. Miller, D.C. Bauer, K.S. Davison, L. Dian, D.A. Hanley, D.L. Kendler, C.K. Yuen, and E.M. Lewiecki. 2013. Bisphosphonate therapy for

- osteoporosis: benefits, risks, and drug holiday. *The American journal of medicine*. 126:13-20.
- Michaille, J.-J., V. Piurowski, B. Rigot, H. Kelani, E.C. Fortman, and E. Tili. 2018. Mir-663, a microRNA linked with inflammation and cancer that is under the influence of resveratrol. *Medicines*. 5:74.
- Mignatti, P., and D.B. Rifkin. 1996. Plasminogen activators and matrix metalloproteinases in angiogenesis. *Enzyme and Protein*. 49:117-137.
- Miksad, R.A., K.-C. Lai, T.B. Dodson, S.-B. Woo, N.S. Treister, O. Akinyemi, M. Bihrl, G. Maytal, M. August, and G.S. Gazelle. 2011. Quality of life implications of bisphosphonate-associated osteonecrosis of the jaw. *The oncologist*. 16:121-132.
- Mizoguchi, F., Y. Murakami, T. Saito, N. Miyasaka, and H. Kohsaka. 2013. miR-31 controls osteoclast formation and bone resorption by targeting RhoA. *Arthritis research & therapy*. 15:R102.
- Mozzati, M., G. Gallesio, V. Arata, R. Pol, and M. Scoletta. 2012. Platelet-rich therapies in the treatment of intravenous bisphosphonate-related osteonecrosis of the jaw: a report of 32 cases. *Oral Oncol*. 48:469-474.
- Nagalingam, R.S., N.R. Sundaresan, M. Noor, M.P. Gupta, R.J. Solaro, and M. Gupta. 2014. Deficiency of cardiomyocyte-specific microRNA-378 contributes to the development of cardiac fibrosis involving a transforming growth factor β (TGF β 1)-dependent paracrine mechanism. *Journal of Biological Chemistry*. 289:27199-27214.
- Nisi, M., F. La Ferla, D. Karapetsa, S. Gennai, M. Miccoli, A. Baggiani, F. Graziani, and M. Gabriele. 2015. Risk factors influencing BRONJ staging in patients receiving intravenous bisphosphonates: a multivariate analysis. *International journal of oral and maxillofacial surgery*. 44:586-591.
- Nissen, N.N., P. Polverini, A.E. Koch, M.V. Volin, R.L. Gamelli, and L.A. DiPietro. 1998. Vascular endothelial growth factor mediates angiogenic activity during the proliferative phase of wound healing. *The American journal of pathology*. 152:1445.

- Nonaka, R., Y. Miyake, T. Hata, Y. Kagawa, T. Kato, H. Osawa, J. Nishimura, M. Ikenaga, K. Murata, and M. Uemura. 2015. Circulating miR-103 and miR-720 as novel serum biomarkers for patients with colorectal cancer. *International journal of oncology*. 47:1097-1102.
- Parfitt, A. 2000. The mechanism of coupling: a role for the vasculature. *Bone*. 26:319-323.
- Parker, L.H., M. Schmidt, S.-W. Jin, A.M. Gray, D. Beis, T. Pham, G. Frantz, S. Palmieri, K. Hillan, and D.Y. Stainier. 2004. The endothelial-cell-derived secreted factor Eglf7 regulates vascular tube formation. *Nature*. 428:754-758.
- Pitari, M.R., M. Rossi, N. Amodio, C. Botta, E. Morelli, C. Federico, A. Gullà, D. Caracciolo, M.T. Di Martino, and M. Arbitrio. 2015. Inhibition of miR-21 restores RANKL/OPG ratio in multiple myeloma-derived bone marrow stromal cells and impairs the resorbing activity of mature osteoclasts. *Oncotarget*. 6:27343.
- Poliseno, L., A. Tuccoli, L. Mariani, M. Evangelista, L. Citti, K. Woods, A. Mercatanti, S. Hammond, and G. Rainaldi. 2006. MicroRNAs modulate the angiogenic properties of HUVECs. *Blood*. 108:3068-3071.
- Pulkkinen, K., T. Malm, M. Turunen, J. Koistinaho, and S. Ylä-Herttuala. 2008. Hypoxia induces microRNA miR-210 in vitro and in vivo. *FEBS letters*. 582:2397-2401.
- Ruggiero, S., T. Dodson, and J. Fantasia. 2014. AAOMS position paper: Medication-related osteonecrosis of the jaw—2014 Update. *American Association of Oral and Maxillofacial Surgeons*.
- Russell, R.G.G. 2011. Bisphosphonates: the first 40years. *Bone*. 49:2-19.
- Santini, D., B. Vincenzi, G. Avvisati, G. Dicuonzo, F. Battistoni, M. Gavasci, A. Salerno, V. Denaro, and G. Tonini. 2002. Pamidronate induces modifications of circulating angiogenetic factors in cancer patients. *Clinical Cancer Research*. 8:1080-1084.
- Santini, D., B. Vincenzi, G. Dicuonzo, G. Avvisati, C. Massacesi, F. Battistoni, M. Gavasci, L. Rocci, M.C. Tirindelli, and V. Altomare. 2003. Zoledronic acid induces significant and long-lasting modifications of circulating angiogenic factors in cancer patients. *Clinical Cancer Research*. 9:2893-2897.
- Somerman, M.J., and L.K. McCauley. 2006. Bisphosphonates: sacrificing the jaw to save the skeleton? *BoneKEy-Osteovision*. 3:12-18.

- Suárez, Y., C. Fernández-Hernando, J. Yu, S.A. Gerber, K.D. Harrison, J.S. Pober, M.L. Iruela-Arispe, M. Merkenschlager, and W.C. Sessa. 2008. Dicer-dependent endothelial microRNAs are necessary for postnatal angiogenesis. *Proceedings of the National Academy of Sciences*. 105:14082-14087.
- Sugatani, T., and K. Hruska. 2007. MicroRNA-223 is a key factor in osteoclast differentiation. *Journal of cellular biochemistry*. 101:996-999.
- Sunycz, J. 2008. Optimizing dosing frequencies for bisphosphonates in the management of postmenopausal osteoporosis: patient considerations. *Clinical interventions in aging*. 3:611.
- Tatsuguchi, M., H.Y. Seok, T.E. Callis, J.M. Thomson, J.-F. Chen, M. Newman, M. Rojas, S.M. Hammond, and D.-Z. Wang. 2007. Expression of microRNAs is dynamically regulated during cardiomyocyte hypertrophy. *Journal of molecular and cellular cardiology*. 42:1137-1141.
- Veikkola, T., and K. Alitalo. 1999. VEGFs, receptors and angiogenesis. *In Seminars in cancer biology*. Vol. 9. Elsevier. 211-220.
- Ventura, A., A.G. Young, M.M. Winslow, L. Lintault, A. Meissner, S.J. Erkeland, J. Newman, R.T. Bronson, D. Crowley, and J.R. Stone. 2008. Targeted deletion reveals essential and overlapping functions of the miR-17~92 family of miRNA clusters. *Cell*. 132:875-886.
- Vescovi, P., G. Campisi, V. Fusco, G. Mergoni, M. Manfredi, E. Merigo, L. Solazzo, M. Gabriele, G.M. Gaeta, and G. Favia. 2011. Surgery-triggered and non surgery-triggered Bisphosphonate-related Osteonecrosis of the Jaws (BRONJ): A retrospective analysis of 567 cases in an Italian multicenter study. *Oral Oncology*. 47:191-194.
- Wagner, E. 2010. Bone development and inflammatory disease is regulated by AP-1 (Fos/Jun). *Annals of the rheumatic diseases*. 69:i86-i88.
- Wang, H.-W., T.-S. Huang, H.-H. Lo, P.-H. Huang, C.-C. Lin, S.-J. Chang, K.-H. Liao, C.-H. Tsai, C.-H. Chan, and C.-F. Tsai. 2014. Deficiency of the microRNA-31-microRNA-720 pathway in the plasma and endothelial progenitor cells from

- patients with coronary artery disease. *Arteriosclerosis, thrombosis, and vascular biology*. 34:857-869.
- Wang, S., A.B. Aurora, B.A. Johnson, X. Qi, J. McAnally, J.A. Hill, J.A. Richardson, R. Bassel-Duby, and E.N. Olson. 2008. The endothelial-specific microRNA miR-126 governs vascular integrity and angiogenesis. *Developmental cell*. 15:261-271.
- Wang, S., and E.N. Olson. 2009. AngiomiRs—key regulators of angiogenesis. *Current opinion in genetics & development*. 19:205-211.
- Wu, F., Z. Yang, and G. Li. 2009. Role of specific microRNAs for endothelial function and angiogenesis. *Biochemical and biophysical research communications*. 386:549-553.
- Würdinger, T., B.A. Tannous, O. Saydam, J. Skog, S. Grau, J. Soutschek, R. Weissleder, X.O. Breakefield, and A.M. Krichevsky. 2008. miR-296 regulates growth factor receptor overexpression in angiogenic endothelial cells. *Cancer cell*. 14:382-393.
- Yang, R., Y. Tao, C. Wang, Y. Shuai, and L. Jin. 2018. Circulating microRNA Panel as a Novel Biomarker to Diagnose Bisphosphonate-Related Osteonecrosis of the Jaw. *International journal of medical sciences*. 15:1694.
- Yoneda, T., H. Hagino, T. Sugimoto, H. Ohta, S. Takahashi, S. Soen, A. Taguchi, T. Nagata, M. Urade, and T. Shibahara. 2017. Antiresorptive agent-related osteonecrosis of the jaw: Position Paper 2017 of the Japanese Allied Committee on Osteonecrosis of the Jaw. *Journal of bone and mineral metabolism*. 35:6-19.
- Zaidi, M., S. Epstein, S.T. Harris, J.D. Kohles, and C.H. Chesnut. 2007. Progression of Efficacy with Ibandronate. *Annals of the New York Academy of Sciences*. 1117:273-282.
- Zandi, M., A. Dehghan, H. Malekzadeh, P. Janbaz, K. Ghadermazi, and P. Amini. 2016. Introducing a protocol to create bisphosphonate-related osteonecrosis of the jaw in rat animal model. *J Craniomaxillofac Surg*. 44:271-278.
- Zhang, Y., R.-l. Xie, C.M. Croce, J.L. Stein, J.B. Lian, A.J. Van Wijnen, and G.S. Stein. 2011. A program of microRNAs controls osteogenic lineage progression by

targeting transcription factor Runx2. *Proceedings of the National Academy of Sciences*. 108:9863-9868.

Zhou, Y., Y. Liu, and L. Cheng. 2012. miR-21 expression is related to particle-induced osteolysis pathogenesis. *Journal of Orthopaedic Research*. 30:1837-1842.



VITA

NAME Thapakorn Surajkulwatana

DATE OF BIRTH 17 Feb 1988

PLACE OF BIRTH Songkhla

INSTITUTIONS ATTENDED Naresuan University

HOME ADDRESS 319/2 Soi 17 Kanjanavanid road Hatyai Songkhla, Thailand

PUBLICATION Interactive VDO conference at The 5th RSU National and International Research Conference on Science and Technology, Social Science and Humanities 2020

